IEEE Access
Multidisciplinary ⋮ Rapid Review ⋮ Open Access Journal

Received 18 March 2024, accepted 19 April 2024, date of publication 6 May 2024, date of current version 15 May 2024.

Digital Object Identifier 10.1109/ACCESS.2024.3397558

TOPICAL REVIEW

Review of Mode Conversion and Modal Analysis in Electromagnetic Compatibility

LUDOVICA ILLIANO, XINGLONG WU, (Senior Member, IEEE), FLAVIA GRASSI, (Senior Member, IEEE), GIORDANO SPADACINI, (Senior Member, IEEE), AND SERGIO A. PIGNARI, (Fellow, IEEE)

Department of Electronics, Information and Bioengineering, Politecnico di Milano, 20133 Milan, Italy

Corresponding author: Xinglong Wu (xinglong.wu@polimi.it)

This study was carried out within the MOST—Sustainable Mobility Center and received funding from the European Union Next-GenerationEU (PIANO NAZIONALE DI RIPRESA E RESILIENZA (PNRR)—MISSIONE 4 COMPONENTE 2, INVESTIMENTO 1.4—D.D. 1033 17/06/2022, CN00000023). This manuscript reflects only the authors' views and opinions, neither the European Union nor the European Commission can be considered responsible for them.

ABSTRACT Undesired conversion between common-mode (CM) and differential-mode (DM) noise often occurs in modern electronic and electrical systems, posing challenges in terms of Electromagnetic Compatibility (EMC). Modal analysis represents a crucial tool in EMC investigation and provides insight into the mechanism underlying mode conversion. By inspecting CM and DM behaviors and their interconversion, it allows for understanding of conducted emission propagation mechanisms, drives electromagnetic interference (EMI) filter design towards optimal/tailored solutions, and enables the possibility to identify the main contributors to the radiated emission phenomenon. This paper offers a comprehensive review of mathematical methodologies and modelling strategies for EMC-oriented modal analysis, with particular emphasis on mode conversion phenomena. To this end, modal decomposition techniques and standard parameters for quantifying mode conversion are summarized and compared. Additionally, the paper provides an overview and in-depth discussion of different scenarios and test cases in which mode conversion occurs, with the final goal to achieve a systematic comprehension of its root causes and consequences within power and communication systems. Eventually, a survey of circuit modelling approaches for mode conversion is presented, offering insights into addressing this phenomenon effectively.

INDEX TERMS Common mode, differential mode, electromagnetic compatibility, mode conversion, multiconductor transmission line (MTL).

I. INTRODUCTION

Electronic and electrical devices may cause interference in nearby units/systems, leading to electromagnetic compatibility (EMC) issues. The generation, coupling, and propagation of electromagnetic (EM) noise are complex phenomena, whose analysis requires a deep understanding not only of the functional part of the system but also of and primarily of its non-ideal behavior, e.g., due to parasitics. As a matter of fact, analysing the functional part of the system only does not allow digging into the root cause of radio-frequency (RF) EM energy emission and reception. This happens for instance when mode conversion occurs, e.g., when the functional differential mode (DM) signal is converted into undesired common mode (CM) noise due to asymmetries affecting different parts of the system. Indeed, in practical structures, the CM noise is ideally null, and signal/power transmission is achieved by resorting to the DM only (see Fig. 1). However, due to imbalance affecting the terminal networks and/or the propagation path, a portion of DM energy can be actually converted into CM noise, thus giving rise to possible phenomena of interference. Such a mechanism of mode conversion is dual. Namely, if a structure is affected by imbalance, not only the functional DM is converted into CM, but also the external CM noise coupled with the structure is converted into DM, making the structure susceptible to the noise generated by nearby devices. A classical example is represented by twisted wire

The associate editor coordinating the review of this manuscript and approving it for publication was Mehmet Alper Uslu.

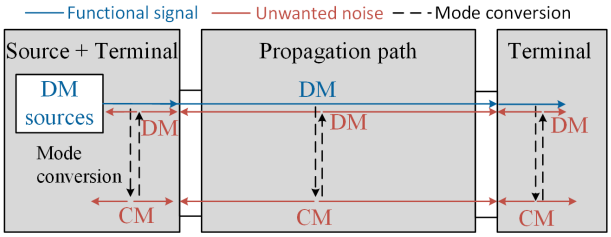

FIGURE 1. Principle drawing of mode conversion in a DM system.

TABLE 1. Modal analysis nomenclature.

	Alternative names
DM	Symmetrical mode, odd mode, normal mode,
CM	Asymmetrical mode, even mode
Mode conversion	Cross mode, mixed mode

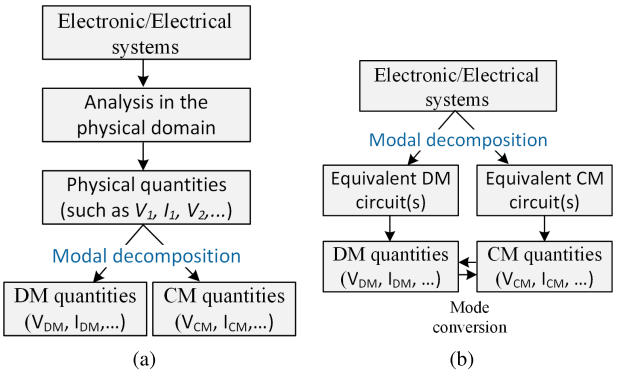

FIGURE 2. General procedures of (a) traditional analysis and (b) modal analysis for electronic/electrical systems.

pairs operated according to DM signalling schemes. In these structures, the DM signal is transmitted as the difference between two complementary signals with respect to ground. Hence, external noise coupled with the wiring structure ideally cancels out, thus making signal transmission ideally interference-free. However, if asymmetries exist (e.g., due to imperfections in the wiring structure or tolerances affecting the terminations), the CM noise is converted into DM noise, which can interfere with the transmissed DM signal with consequent degradation and even failure of signal transmission. The literature addressing modal analysis and mode conversion is extensive, and it is worth mentioning that there exist various definitions and names used to denote modal quantities, as summarized in Tab. 1.

For assessing DM/CM quantities, the traditional approach involves computing physical quantities (such as line voltages/currents V_1, I_1, etc.) in the physical domain as the first step. These physical quantities are subsequently transformed into modal quantities through modal decomposition, as depicted in Fig. 2(a). However, such an approach fails to explicitly highlight whether mode conversion has occurred, since it provides the overall CM and DM quantities only. This information is undeniably useful, for instance, to select a proper Electromagnetic Interference (EMI) filter (a posteriori solution, requiring additional costs). However, it does not usually provide the information required to improve the design of the system so that the additional noise generated by mode conversion can be directly mitigated by adopting proper design strategies.

To effectively analyze mode conversion thus unveiling the mechanism of generation and propagation of undesired CM/DM noise, the alternative approach is to transform and directly analyze the system in the modal domain. This leads to system decomposition into modal equivalent circuits (e.g., a CM and a DM circuit in the canonical case of three-wire structures), which clearly put in evidence the geometrical/electrical parameters affecting each mode. In the absence of mode conversion, modal circuits are uncoupled and can be solved independently. Conversely, if the system is affected by imbalance, the resulting mode conversion and the geometrical and electrical parameters determining it result to be clearly highlighted by the modal circuits, which are no longer decoupled in the modal domain (see Fig. 2(b)). For this reason, resorting to modal analysis and equivalent modal circuits represents a fundamental tool for EMC engineers, as it offers a deep insight to understand the underlying mechanism of generation of undesired noise, and enables the development of guidelines for EMC-oriented design.

The objective of this work is to provide a comprehensive overview on state-of-the-art studies on modal analysis and mode conversion targeted at EMC analyses. In particular, in Sec.II, the mathematical basis of modal decomposition is reviewed, with the objective to explain and summarize the different definitions of modal quantities available in the literature. Common metrics for mode conversion exploited in technical papers and international standards are recalled in Sec. III. An overview on different structures in which mode conversion may arise is presented in Sec. IV. A detailed literature review on the methods developed to analyse mode conversion in these structures is provided in Sec. V, VI and VII. Specifically, in Sec. V, the methods used to analyze the impact of mode conversion on terminal networks are summarized, with a focus on designing terminations for signal and power circuits. Sec. VI provides a survey of studies on mode conversion in transmission lines, structured into three categories: cables, PCB traces, and lumped discontinuities. In Sec. VII, other methods for the analysis of mode conversion pertaining to structures not classified in the previous categories are presented. Furthermore, a summarized analysis of modelling techniques for mode conversion is provided in Sec. VIII. Finally, conclusions are drawn in Sec. IX.

II. MODAL DECOMPOSITION

From the mathematical viewpoint modal analysis consists in a change of variables achieved through the application of similarity transformation matrices to decouple systems of coupled equations. In EMC analyses, similarity

transformation matrices are employed to solve multiconductor transmission line (MTL) equations, resulting in the definition of a set of uncoupled propagation modes. Decoupling the second-order Telegrapher equations by a proper similarity transformation matrix is enough for solution purposes. However, if the objective is to also decouple first-order equations (e.g., to derive equivalent modal circuits), a pair of transformation matrices, $\mathbf{T}_{VmN}$ and $\mathbf{T}_{ImN}$, concurrently diagonalizing both the per unit length (p.u.l.) impedance and admittance matrices, $\mathbf{Z}$ and $\mathbf{Y}$, should be identified. By employing similarity transformation matrices, physical quantities are redefined in terms of known modal quantities. For EMC analyses, the most commonly used transformation matrices are those directly derived from the definitions of DM and CM currents and voltages. DM and CM are the counterparts of the odd and even modes primarily used in microwave sector to describe the propagation modes in pairs of strip lines and microstrip lines. In physical terms, CM/even mode excitation occurs when the currents flowing in the two wires of the transmission line pair are of equal magnitude and propagate in the same direction, while DM/odd mode excitation occurs when the two currents are still of equal magnitude, but propagate in opposite directions.

The introduction of CM and DM quantities allows for a simpler identification of the dominant effect involved in an interference phenomenon, which is a key ingredient for the design of proper mitigation strategies. Consider a generic $(N+1)$-conductor system consisting of N signal conductors and a reference ground. The vectors collecting physical voltages $\mathbf{V} = [V_1, \ldots, V_N]$ and currents $\mathbf{I} = [I_1, \ldots, I_N]$ are converted into the corresponding modal vectors $\mathbf{V}_m$, $\mathbf{I}_m$ as:

$$\mathbf{V}_m = \begin{bmatrix} V_{CM} \\ V_{DM1} \\ \vdots \\ V_{DM(N-1)} \end{bmatrix} = \mathbf{T}_{VmN} \cdot \begin{bmatrix} V_1 \\ V_2 \\ \vdots \\ V_N \end{bmatrix}$$

$$\mathbf{I}_m = \begin{bmatrix} I_{CM} \\ I_{DM1} \\ \vdots \\ I_{DM(N-1)} \end{bmatrix} = \mathbf{T}_{ImN} \cdot \begin{bmatrix} I_1 \\ I_2 \\ \vdots \\ I_N \end{bmatrix} \tag{1}$$

where V_{CM}, I_{CM} and V_{DMx}, I_{DMx} $(x = 1, \ldots, N-1)$ denote CM and DM voltages and currents, respectively, and $\mathbf{T}_{VmN}$ and $\mathbf{T}_{ImN}$ are suitable similarity transformation matrices. Employing the modal transformation in (1), modal (p.u.l.) impedance and admittance matrices, $\mathbf{Z}_m$ and $\mathbf{Y}_m$ respectively, can be deduced as follows. Consider the impedance matrix $\mathbf{Z}$. The relationship between the voltage vector $\mathbf{V}$ and the current vector $\mathbf{I}$ in terms of physical quantities reads:

$$f(\mathbf{V}) = g(\mathbf{Z})k(\mathbf{I}). \tag{2}$$

where f, g, k are linear operators. Applying (1) to (2) gives:

$$f(\mathbf{T}_{VmN}^{-1}\mathbf{V}_m) = g(\mathbf{Z})k(\mathbf{T}_{ImN}^{-1}\mathbf{I}_m). \tag{3}$$

Multiplying both sides of (3) by T_{VmN} yields

$$f(\mathbf{V}_m) = g(\mathbf{Z}_m)k(\mathbf{I}_m), \tag{4}$$

with the modal impedance Z_m taking the expression

$$\mathbf{Z}_m = \mathbf{T}_{VmN}\mathbf{Z}\,\mathbf{T}_{ImN}^{-1}. \tag{5}$$

As stated in [1], on condition that the system exhibits certain symmetries, it is possible to identify a (or multiple) pair of $\mathbf{T}_{VmN}$ and $\mathbf{T}_{ImN}$ matrices, able to diagonalize the TL's first order equations, and, as a consequence, also the impedance matrix $\mathbf{Z}$. In these cases, similarity transformation matrices can be obtained from the solution of an eigenvalue problem, defined as

$$det(\mathbf{Z} - \lambda\mathbf{I}) = 0. \tag{6}$$

Let's assume that, according to the common practice, the transformation matrices $\mathbf{T}_{VmN}$ and $\mathbf{T}_{ImN}$ are defined for the most ideal wiring configuration ensuring signal integrity in the application of interest, that is, for a perfectly balanced MTL whose cross-section is geometrically symmetric with respect to the reference conductor. Accordingly the ideal modal impedance matrix $\mathbf{Z}_m$ is diagonal,

$$\mathbf{Z}_m^{ideal} = \begin{bmatrix} Z_{\mathrm{CM}} & 0 & \ldots & 0 \\ 0 & Z_{DM1} & \ldots & 0 \\ \vdots & \vdots & \ddots & \vdots \\ 0 & 0 & \ldots & Z_{DM(N-1)} \end{bmatrix}, \tag{7}$$

which means that the N modes are fully uncoupled and mode conversion does not occur. If the same matrices $\mathbf{T}_{VmN}$ and $\mathbf{T}_{ImN}$ are applied to an unbalanced system (whose imbalance arises for any non-ideal effect), the elements outside the main diagonal are no longer null, due to non-negligible interactions among modes. In this context, expanding the matrix $\mathbf{Z}_m$ gives

$$\mathbf{Z}_m = \begin{bmatrix} Z_{\mathrm{CM}} & Z_{\mathrm{CD1}} & \ldots & \ldots & Z_{\mathrm{CD(N-1)}} \\ Z_{\mathrm{D1C}} & Z_{DM1} & Z_{D1D2} & \ldots & Z_{D1D(N-1)} \\ Z_{\mathrm{D2C}} & Z_{D2D1} & Z_{DM2} & \ldots & Z_{D2D(N-1)} \\ \vdots & \vdots & \vdots & \ddots & \vdots \\ Z_{\mathrm{D(N-1)C}} & Z_{D(N-1)D1} & \ldots & \ldots & Z_{DM(N-1)} \end{bmatrix}, \tag{8}$$

where Z_{CM} and Z_{DMi} are the CM and i-th DM equivalent impedances, respectively, Z_{CDi} and Z_{DiC} are the impedances representing the mode conversions from the CM to the i-th DM, and from the i-th DM to the CM, respectively, and Z_{DiDj} accounts for the mutual impedance coupling between the i-th and j-th DM circuits. In this way, modal structure parameters, i.e. impedances in the DM and CM equivalent circuits, are obtained and the parameters accounting for mode conversion can be observed. Similar reasoning can be applied to $\mathbf{Y}_m$, which is equal to:

$$\mathbf{Y}_m = \mathbf{T}_{ImN}\mathbf{Y}\mathbf{T}_{VmN}^{-1}. \tag{9}$$

Once the modal quantities are known, physical quantities can be retrieved by applying the inverse transformations. The transformation matrices commonly used to define CM and DM quantities can be interpreted as a special case of similarity transformation matrices, assuring decoupling of both first and second-order MTL equations on condition the system under analysis satisfies specific properties of symmetry with respect to the reference ground.

A. THREE-CONDUCTOR SYSTEMS

Three-conductor systems are widely exploited in electrical and electronic systems. Single-phase/DC power systems including phase/positive, neutral/negative and ground wires are examples of wiring structures used for power supply. Differential signalling circuits involving two complementary signal lines and a reference ground are examples of three-conductor systems widely used for signal transmission. For these structures, one CM and one DM are introduced. The actual definition and corresponding similarity transformation matrices can take slightly different expressions in the literature. For instance, in [2] and [3], the $\mathbf{T}_{Vm2}$ and $\mathbf{T}_{Im2}$ are defined as

$$\mathbf{T}_{Vm2} = \mathbf{T}_{Im2} = \begin{bmatrix} 1/2 & 1/2 \\ 1/2 & -1/2 \end{bmatrix}, \tag{10}$$

while in [4], they are introduced as

$$\mathbf{T}_{Vm2_2} = \begin{bmatrix} 1/2 & 1/2 \\ 1 & -1 \end{bmatrix}; \quad \mathbf{T}_{Im2_2} = \begin{bmatrix} 1 & 1 \\ 1/2 & -1/2 \end{bmatrix}. \tag{11}$$

Although these definitions lead to slightly different equivalent modal circuits, they are actually equivalent as it will be proven by recalling MTL theory. A three-conductor system balanced with respect to the reference wire, is characterized by a symmetric p.u.l. impedance matrix $\mathbf{Z}_2$

$$\mathbf{Z}_2 = \begin{bmatrix} z & z_{12} \\ z_{12} & z \end{bmatrix}. \tag{12}$$

For such systems, the solution of the eigenvalue problem reads:

$$det(\mathbf{Z}_2 - \lambda \mathbf{I}) = 0, \tag{13}$$

where λ is the eigenvalue vector and $\mathbf{I}$ is the identity matrix. Solution of (13) leads to two eigenvalues i.e., $\lambda_{1,2} = z \pm z_{12}$. Solving the problem at the eigenvalues provides an eigenvector matrix $\mathbf{T}_{eig2}$:

$$\mathbf{T}_{eig2} = \begin{bmatrix} 1 & 1 \\ 1 & -1 \end{bmatrix}, \tag{14}$$

that satisfies

$$\mathbf{T}_{eig2}^{-1}\mathbf{Z}_2\mathbf{T}_{eig2} = \begin{bmatrix} z + z_{12} & 0 \\ 0 & z - z_{12} \end{bmatrix}. \tag{15}$$

It is straightforward to notice that (10) decouples CM and DM by recognizing that $\mathbf{T}_{eig2}^{-1} = \mathbf{T}_{Vm2} = \mathbf{T}_{Im2}$. Substituting the modal decomposition in (11) into (5), it is verified that:

$$\mathbf{Z}_{m2_2} = \mathbf{T}_{Vm2_2}\mathbf{Z}_2\mathbf{T}_{Im2_2}^{-1} = \begin{bmatrix} (z + z_{12})/2 & 0 \\ 0 & 2 \cdot (z - z_{12}) \end{bmatrix}. \tag{16}$$

It is possible to define several similarity transformation matrices starting from (15). Indeed, they can be obtained as linear combination of the eigenvectors associated with the eigenvalues in (15), i.e.,

$$\mathbf{T}_{Vm2_2} = \mathbf{X} \cdot \mathbf{T}_{eig2}^{-1}; \quad \mathbf{T}_{Im2_2}^{-1} = \mathbf{T}_{eig2} \cdot 0.5\mathbf{X}, \tag{17}$$

where $\mathbf{X} = \begin{bmatrix} 1 & 0 \\ 0 & 2 \end{bmatrix}$ is a diagonal matrix. $\mathbf{T}_{Vm2_2}$ and $\mathbf{T}_{Im2_2}$ also diagonalize the $\mathbf{Y}$ matrix. Although the application of different transformations lead to equivalent modal circuits with slightly different values of the involved circuit components, the intrinsic properties of the system are not affected, since modal transformations only change the system coordinates. As a consequence, as long as the same transformation is consistently applied to all components in the network, the evaluation of relevant quantities (e.g., the evaluation of modal insertion loss of an EMI filter) is not affected by the specific transformation matrix.

B. FOUR-CONDUCTOR SYSTEMS

Four-conductor systems are widely exploited in power distribution systems and include three active lines and a reference/ground line. In these structures, one CM and two DMs can be introduced as shown in the following. Let's consider a perfectly balanced four-wire system characterized by the impedance matrix

$$\mathbf{Z}_3 = \begin{bmatrix} z & z_{12} & z_{12} \\ z_{12} & z & z_{12} \\ z_{12} & z_{12} & z \end{bmatrix}. \tag{18}$$

Solution of the eigenvalues problem $(\mathbf{Z}_3 - \lambda\mathbf{I})\mathbf{v} = \mathbf{0}$ yields two distinct eigenvalues, i.e. $\lambda_1 = z + 2z_{12}$ of algebraic multiplicity 1 and $\lambda_{2,3} = z - z_{12}$ of algebraic multiplicity 2 with associated eigenvectors $[\mathbf{v_1}, \mathbf{v_2}, \mathbf{v_3}]$, which in compact form read

$$\mathbf{T}_{eig3} = [\mathbf{v_1}, \mathbf{v_2}, \mathbf{v_3}] = \begin{bmatrix} 1 & 0 & 1 \\ 1 & 1 & 0 \\ 1 & -1 & -1 \end{bmatrix}. \tag{19}$$

The first eigenvector $\mathbf{v_1}$, associated with λ_1, leads to the definition of the CM, whereas the eigenvectors $[\mathbf{v_2}, \mathbf{v_3}]$, associated with $\lambda_{2,3}$, lead to the definition of the two DMs. By definition, the eigenvector matrix in (19) makes the impedance matrix $\mathbf{Z}_3$ in (18) diagonal, i.e.,

$$\mathbf{Z}_{m3} = \mathbf{T}_{eig3}^{-1}\mathbf{Z}_3\mathbf{T}_{eig3} = \begin{bmatrix} z + 2z_{12} & 0 & 0 \\ 0 & z - z_{12} & 0 \\ 0 & 0 & z - z_{12} \end{bmatrix}. \tag{20}$$

The comparison of (20) and (5) leads to $\mathbf{T}_{eig3}^{-1} = \mathbf{T}_{Vm3} = \mathbf{T}_{Im3}$. The inverse matrix $\mathbf{T}_{eig3}^{-1}$ corresponds to the modal

transformation matrix obtained considering each physical voltage (V_1,V_2, or V_3) as the sum of DM and CM voltages [5]. The modal transformation matrix $\mathbf{T}_{Vm3}$ is:

$$\mathbf{T}_{Vm3} = \mathbf{T}_{eig3}^{-1} = \frac{1}{3}\begin{bmatrix} 1 & 1 & 1 \\ 2 & -1 & -1 \\ -1 & 2 & -1 \end{bmatrix}. \tag{21}$$

Alternative pairs of similarity transformation matrices $\mathbf{T}_{Vm3_2}$ and $\mathbf{T}_{Im3_2}$ can be obtained considering linear combinations of the eigenvectors. A noteworthy example is the Fortescue transformation matrix widely used in the analysis of power systems for the so-called symmetrical components decomposition [6]:

$$\mathbf{T}_{Vm3_2} = \begin{bmatrix} 1 & 1 & 1 \\ 1 & e^{j2\pi/3} & e^{j4\pi/3} \\ 1 & e^{j4\pi/3} & e^{j2\pi/3} \end{bmatrix}. \tag{22}$$

According to (22), three-phase voltages (V_1, V_2 and V_3) are converted into the corresponding zero, positive and negative sequence quantities, and the obtained single-phase equivalent circuits (sequence circuits) are exploited for fault analyses.

C. ($N+1$)-CONDUCTOR SYSTEMS ($N > 3$)

For systems involving more than three signal lines, there is no definition of modal decomposition which is widely accepted in the literature. Various modal decompositions can be formulated so as to point out different kinds of compositions of CM and DM quantities, as seen in previous examples.

A significant definition of modal decomposition results from considering CM component as the sum of all physical quantities, as direct extension of the definitions in Sec. II-B. This choice is relevant for EMC analyses, as it allows computing the net (CM) current flowing through the loop composed by all the wires in a bundle and the return metallic ground. This approach is widely used to investigate radiated emissions [7], as well as radiated/conducted susceptibility problems [8], [9]. Suitable similarity transformation matrices retaining such a CM definition can be derived, as discussed in Sec. II-A and Sec. II-B, through the solution of the eigenvalue problem. For instance, for a system comprising $N+1$ conductors, the corresponding transformation matrices $\mathbf{T}_{VmN}$ and $\mathbf{T}_{ImN}$ can be introduced as:

$$\mathbf{T}_{VmN} = \mathbf{T}_{ImN} = \frac{1}{N}\cdot\begin{bmatrix} 1 & 1 & \dots & 1 \\ -1 & (N-1) & \dots & -1 \\ \vdots & \vdots & \ddots & \vdots \\ -1 & -1 & \dots & (N-1) \end{bmatrix} \tag{23}$$

An application example of a variant of (23) is given in [10]. The work considers two adjacent differential lines (DLs) above ground (see: Fig. 3). The goal of [10] was to predict the radiation from the whole system involving the two DLs. This decomposition involves only one CM mode,

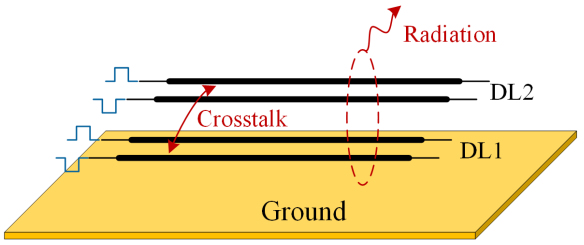

FIGURE 3. Two differential lines above ground and EMC problems related to CM noise.

as depicted in (23):

$$\begin{bmatrix} V_{CM} \\ V_{DM1} \\ V_{DM2} \\ V_{DM3} \end{bmatrix} = \begin{bmatrix} 1/4 & 1/4 & 1/4 & 1/4 \\ 1 & -1 & 0 & 0 \\ 0 & 0 & 1 & -1 \\ 1/2 & 1/2 & -1/2 & -1/2 \end{bmatrix} \cdot \begin{bmatrix} V_1 \\ V_2 \\ V_3 \\ V_4 \end{bmatrix} \tag{24}$$

On the other hand, if the objective of the analysis is to examine EMC issues within the system involving several sets of differential signalling, it is possible to partition the system into several subsets of three-conductor systems and to subsequently apply the canonical modal decompositions defined in (10) or (11). An example of application of this method is the generalization of mixed-mode S-parameters [11], which has gained importance in multi-wire/trace analyses, as demonstrated in [12] and [13]. Implementing the same definition, [14] investigated crosstalk and co-existing problems of the two DLs in Fig. 3. Therefore, the two DLs were considered separately, leading to the identification of two CMs:

$$\begin{bmatrix} V_{CM1} \\ V_{DM1} \\ V_{CM2} \\ V_{DM2} \end{bmatrix} = \begin{bmatrix} \mathbf{T}_{Vm2_2} & \mathbf{0}_{2\times2} \\ \mathbf{0}_{2\times2} & \mathbf{T}_{Vm2_2} \end{bmatrix} \cdot \begin{bmatrix} V_1 \\ V_2 \\ V_3 \\ V_4 \end{bmatrix} \tag{25}$$

Both the aforementioned options can be applied in general EMC analysis, but one may be preferable than the other depending on the goal of the analysis. In particular, (23) and (24) are more suitable for radiated and susceptibility analyses, while (25) is more efficient for intra-system compatibility assessment.

III. METRICS FOR MODE CONVERSION

To quantify mode conversion, starting from the modal decomposition presented in Sec. II, several metrics have been defined in the literature, which will be reviewed in this Section.

A. MIXED-MODE S-PARAMETERS

Scattering parameters (S-parameters) are widely used for the characterization of multi-port networks. Specifically, to characterize a network in terms of CM and DM quantities a specific set of S-parameters has been introduced in [4], which are known as mixed-mode S-parameters. The transformation from standard four-port single-ended S-parameters to mixed-mode S-parameters was introduced in [15] and [16]. Then,

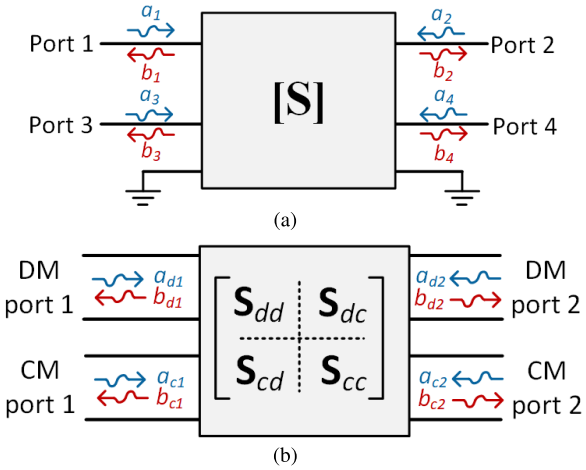

FIGURE 4. S-parameter analysis: (a) Port definition used in this paper and (b) Mixed-mode S-parameter.

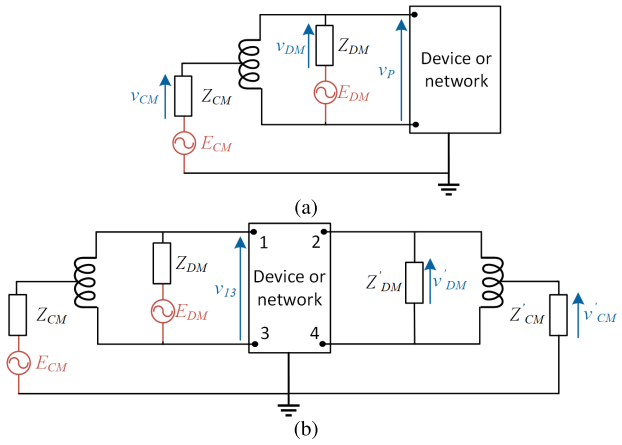

FIGURE 5. Transverse and longitudinal conversion measurement setup recommended by ITU: (a) TCL/LCL (b) TCTL/LCTL.

in [11], the mixed-mode S-parameter theory has been extended to general multiport networks involving CM, DM and single-ended ports. Since the theory was originally developed for a four-port network [4], without loss of generality, in the following we will consider this case with port assignment defined as [16] (see: Fig. 4(a)). Based on (11), after some algebra [11], [16], the mixed-mode S-parameters matrix $\mathbf{S}_{mm}$ is obtained from the S-parameters matrix $\mathbf{S}$ by applying the transformation:

$$\mathbf{S}_{mm} = \mathbf{T}\mathbf{S}\mathbf{T}^{-1} = \begin{bmatrix} \mathbf{S}_{dd} & \mathbf{S}_{dc} \\ \mathbf{S}_{cd} & \mathbf{S}_{cc} \end{bmatrix}, \tag{26}$$

where $\mathbf{T}$ is defined as:

$$\mathbf{T} = \frac{1}{\sqrt{2}} \begin{bmatrix} 1 & 0 & -1 & 0 \\ 0 & 1 & 0 & -1 \\ 1 & 0 & 1 & 0 \\ 0 & 1 & 0 & 1 \end{bmatrix}. \tag{27}$$

It is worth noting that the exact expression in (27) slightly varies depending on port assignment [15], [16]. The 2 × 2 sub-matrices $\mathbf{S}_{dd}$, $\mathbf{S}_{dc}$, $\mathbf{S}_{cd}$ and $\mathbf{S}_{cc}$ represent DM-in-DM-out, CM-in-DM-out, DM-in-CM-out, and CM-in-CM-out S-parameters, respectively. Obviously, as shown in Fig.4(b), $\mathbf{S}_{dd}$ and $\mathbf{S}_{cc}$ are associated with DM ($a_{\{d1,d2\}}$->$b_{\{d1,d2\}}$) and CM ($a_{\{c1,c2\}}$->$b_{\{c1,c2\}}$) propagation; while $\mathbf{S}_{cd}$ and $\mathbf{S}_{dc}$ characterize DM-to-CM ($a_{\{d1,d2\}}$->$b_{\{c1,c2\}}$) and CM-to-DM ($a_{\{c1,c2\}}$->$b_{\{d1,d2\}}$) conversion. Specifically, the DM-to-CM conversion $\mathbf{S}_{cd}$ and CM-to-DM conversion $\mathbf{S}_{dc}$ are

$$\mathbf{S}_{cd} = \begin{bmatrix} S_{c1d1} & S_{c1d2} \\ S_{c2d1} & S_{c2d2} \end{bmatrix}; \quad \mathbf{S}_{dc} = \begin{bmatrix} S_{d1c1} & S_{d1c2} \\ S_{d2c1} & S_{d2c2} \end{bmatrix}, \tag{28}$$

where $\mathbf{S}_{cxdy} = \mathbf{S}_{dycx}$ $(x, y = 1, 2)$ if the structure under analysis is reciprocal. A higher value of $\mathbf{S}_{cxdy}$/$\mathbf{S}_{dycx}$ indicates larger mode conversion and worse EMC performance. The mixed-mode S-parameter measurement is directly allowed by four-port vector network analyzers (VNAs).

B. TRANSVERSE AND LONGITUDINAL CONVERSION (TRANSFER) LOSSES (TCL, LCL, TCTL, AND LCTL)

In order to quantify the degree of imbalance about earth, the International Telecomunication Union (ITU) defines the transverse and longitudinal conversion loss parameters (*TCL* and *LCL*) and the transverse and longitudinal conversion transfer loss parameters (*TCTL* and *LCTL*) in its recommendations [17], [18]. The definitions of *TCL* and *LCL* are based on Fig. 5(a). Specifically, *TCL* and *LCL* are measures of the undesired CM and DM noise introduced by the DM (E_{DM}) and CM (E_{CM}) sources at the same port, as

$$\begin{aligned} TCL &= 20\log_{10}\left|\frac{v_p}{v_{CM}}\right| \text{ dB (with } E_{CM} \text{ off)} \\ LCL &= 20\log_{10}\left|\frac{E_{CM}}{v_{DM}}\right| \text{ dB (with } E_{DM} \text{ off).} \end{aligned} \tag{29}$$

Therefore, *TCL* and *LCL* quantify near-end DM-to-CM and CM-to-DM conversions, respectively. The general relationship between $\mathbf{S}_{c1d1}$/$\mathbf{S}_{d1c1}$ and *TCL*/*LCL* is derived in [19] considering different values of terminal impedances. Similarly, *TCTL* and *LCTL* assess the level of far-end DM-to-CM and CM-to-DM conversion, respectively. Specifically, based on the setup shown in Fig. 5(b), the *TCTL* and *LCTL* are defined between the two ports as:

$$\begin{aligned} TCTL &= 20\log_{10}\left|\frac{v_{13}}{v'_{CM}}\right| \text{ dB (with } E_{CM} \text{ off)} \\ LCTL &= 20\log_{10}\left|\frac{E_{CM}}{v'_{DM}}\right| \text{ dB (with } E_{DM} \text{ off).} \end{aligned} \tag{30}$$

In Fig. 5(a) and Fig. 5(b), the centre-tapped coils (with ideally lossless infinite-inductance) are usually implemented by using baluns [20].

It is worth mentioning that in some applications, especially for the evaluation of cable performance [21], [22], TCL/LCL/TCTL/LCTL are defined as the inverse of the

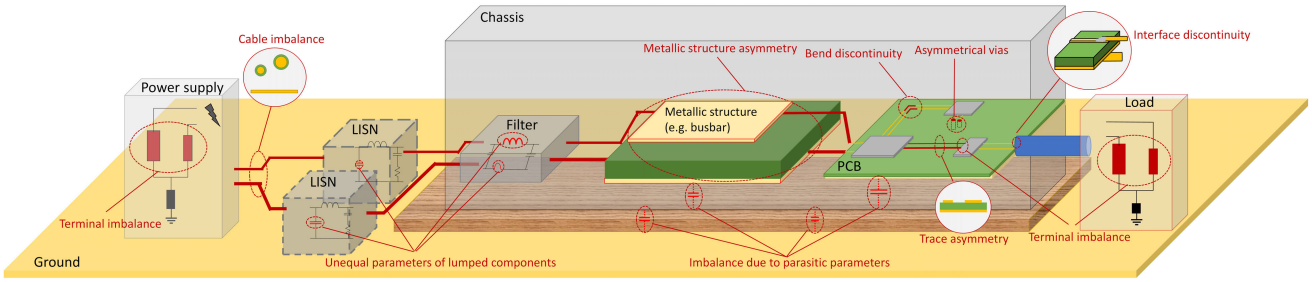

FIGURE 6. Conceptual drawing of common causes of mode conversion in electrical/electronic systems. The causes are highlighted in red.

corresponding mixed-mode S-parameters, namely:

$$TCL_c = -S_{c1d1}|_{dB};\quad LCL_c = -S_{d1c1}|_{dB}$$
$$TCTL_c = -S_{c2d1}|_{dB};\quad LCTL_c = -S_{d2c1}|_{dB}. \tag{31}$$

where port 1-3 provides CM and DM excitation. Similar equations can be written for port 2-4 as excitation port. When the structure under analysis is reciprocal $TCL_c/TCTL_c = LCL_c/LCTL_c$. This is usually true when cabling system is considered. Furthermore, these parameters can be easily measured by using VNAs, providing a balun-free solution. However, compared to previous definitions in (29) and (30), the condition implicitly assumed in (31) is the use of a 50 Ω reference resistance, which means $Z_{DM} = 100\ \Omega$ and $Z_{CM} = 25\ \Omega$. According to this assumption, the following equations also hold true:

$$LCL = LCL_c;\ LCTL = LCTL_c. \tag{32}$$

Unlike (32), there is no strict relationship between $TCL/TCTL$ and $TCL_c/TCTL_c$ since the source definition is different. Based on (29), (30) and (31), a larger value of TCL/LCL/TCTL/LCTL indicates a lower mode conversion. Indeed, cable manufacturers and standards [23] usually provide/require minimum values of these parameters to quantify the worse mode conversions.

C. CM/DM REJECTION RATIO (CMRR/DMRR)

Another parameter used to quantify mode conversion is the CM rejection ratio (CMRR). The CMRR denotes the system ability to reject the CM noise entering at the input of a differential port, thereby it is a valuable measure of CM-to-DM conversion. It was originally introduced to measure the ratio of DM and CM gains of operational amplifiers, and it is ideally infinite. For EMC applications, the CMRR is employed to assess mode conversion in both power converter systems [24] and differential signalling systems [25], [26]. Slightly different definitions of CMRR are available, but it is generally introduced as the ratio between one CM voltage ($\mathcal{V}_{CM}$) and the induced DM voltage ($\mathcal{V}_{DM}$) evaluated at the differential port input:

$$\text{CMRR} = 20\log_{10}\left(\frac{|\mathcal{V}_{CM}|}{|\mathcal{V}_{DM}|}\right)\text{dB}. \tag{33}$$

The larger CMRR the smaller CM-to-DM conversion, thus ensuring signal integrity (SI) performance [27]. A different definition of CMRR, evaluated as the ratio of modal powers instead of voltages, is reported in [28]. CMRR dual is the DM Rejection Ratio (DMRR), defined in [29], which is related to DM-to-CM assessment.

D. OTHER METRICS

In the literature, there exist also other parameters with similar meaning. For instance, [30] quantified the mode conversion using the transfer impedance giving the relationship between CM/DM signals. This is similar to mixed-mode S-parameter, yet is more straightforward for low-frequency analysis. Furthermore, in several EMC analyses, mode conversion is not explicitly quantified by using the above metrics, but it is indirectly assessed by the evaluation of its effects, i.e., in terms of eye diagram degradation [31] or radiated emissions [32].

The metrics presented in this section can be fruitfully used to provide a quantitative estimation of the amount of mode conversion. They can be used by the designer to run comparisons among different realizations of the same system, so to easily identify the configurations assuring better performance in terms of mitigation of mode conversion. Also, specific recommendations in terms of allowable values exist, but they are strongly dependent on the specific application and standards. For instance, the IEEE 802.3 [22] and ISO/IEC 11801 [23] specify different limits in terms of TCL and TCTL[1] for different cabling systems.

IV. OVERVIEW OF MODE CONVERSION IN ELECTRICAL/ELECTRONIC SYSTEMS

Before delving into the details of mode conversion in specific parts of the systems, it is worth providing an overview of mode conversion in the whole system. Indeed, although the components and the interconnections of electrical/electronic systems can vary in different applications, there exist several important structures which are critical for mode conversion from the EMC viewpoint. Fig. 6 provides a conceptual drawing of a system including the key structures possibly

[1]Some limits are specified in terms of the so-called equal level TCTL (ELTCTL) rather than TCTL. ELTCTL = TCTL − IL_{DM} where IL_{DM} is the DM insertion loss of the cable [21].

generating mode conversion. To begin with, mode conversion may occur due to the power supply: the system power supply port is indeed a terminal for high-frequency noise, and therefore it can introduce additional noise due to mode conversion if it is not balanced. In many standard EMC tests, line impedance stabilization networks (LISNs) are placed between the power supply and the system to provide a controlled impedance to the system's power cord outlet, to block interference coming from the power supply, and to provide a proper port for measuring conducted emissions [2]. Therefore, the presence of the LISN can mask the aforesaid power supply imbalance. However it may in turn introduce mode conversion due to its own unbalanced structure. Transmission lines (cables and PCB traces) are the most commonly used interconnections in electrical/electronic systems, but their unbalance is almost unavoidable. Mode conversion may also occur in the presence of asymmetrical discontinuities (e.g., the interfaces between different transmission lines or sharp changes in line layouts) in the propagation path. Furthermore, when the EM energy reaches the load, possible imbalance affecting the loads may cause mode conversion and introduce additional noise. EMI filters themselves, although intended to mitigate conducted emissions, can act as sources of accidental mode conversion. Eventually, unintentional parasitic paths, not meant for functional EM propagation, should also be considered from the EMC viewpoint. Indeed, any metallic structure in the propagation path of the EM energy may introduce additional mode conversion and worsen EMC performance of the system at some specific frequencies. Common examples of unintended routes are the chassis and the air gaps (acting as, for instance, parasitic capacitors between the system and the earth ground). A detailed discussion of mode conversion in each part will be given in the following sections.

V. MODE CONVERSION DUE TO TERMINAL NETWORKS

To avoid mode conversion it is a best practice to design perfectly balanced terminations. In differential signalling systems, terminals are ideally perfectly balanced; therefore, DM-to-CM conversion of differential signals and CM-to-DM conversion of external EM disturbances are theoretically null. Indeed, high-speed signalling designs usually intentionally control the balance terminal conditions at working frequencies to guarantee high SI and EMC performance. However, imbalance frequently occurs in practical situations due to manufacturing uncertainties and non-ideal behavior of components. The resulting CM-to-DM and DM-to-CM conversions due to terminal imbalance were investigated in [25] and [33], respectively.

Unlike terminals in high-speed signalling design, power supply terminals are designed for the propagation of DC or 50/60 Hz power. Hence, they are not designed to assure balance at high-frequencies, and may introduce a significant imbalance from the EMC viewpoint. Reference [34] investigated mode conversion due to terminals in a power-line-communication system. In [32], it has been proved that an unbalanced termination for main power cables can introduce mode conversion even at points remote from the DUT, which may significantly increase the EM emissions of the system. The level of unbalance also depends on the local electricity supply network, which introduces measurement uncertainty in EMC tests. Indeed, an international inter-laboratory comparison shows that the maximum standard deviation of radiated emission measurement can be over 9 dB in the frequency range from 30 MHz to 150 MHz [35]. This uncertainty can be reduced by using common mode absorption devices (CMADs) [36], [37] or very-high-frequency (VHF)[2] LISNs [38]. In some cases [39], VHF-LISNs worked better than CMADs due to the fact that CMAD can suppress the CM noise only. The use of a balanced VHF-LISN can reduce measurement uncertainty but may lead to the measurement of conducted emissions inherently lower than real-world emissions, since perfect balanced terminals (i.e. zero mode conversion) are rare in practice. To overcome this limitation, unbalanced VHF-LISNs have been recently proposed [28], [40]. To account for possible mode conversion during the measurement it was shown that unbalanced VHF-LISNs can both control measurement uncertainty and give worst-case prediction of real-world emissions from a power line communication system [28]. A comprehensive experimental investigation on the comparison between balanced and unbalance VHF-LISNs is provided in [41].

Although the use of a LISN can limit the uncertainty within the tolerance defined by EMC standards, when two or more LISNs are used in the same setup, the variability (due to tolerances) of LISN components may introduce a mismatch of input impedances with consequent mode conversion. For instance, for conducted emission measurement, CISPR 25 [42] requires the use of two LISNs with impedance tolerance $\pm$ 20%. In [30], it was shown that this tolerance could introduce non-negligible differences in the measure of CM conducted-emission in the frequency range from 150 kHz to 2 MHz, due to DM-to-CM conversion.

VI. MODE CONVERSION IN TRANSMISSION LINES

Interconnections (cables and PCB traces) are fundamental in electrical and electronic systems. In these structures, asymmetries, nonuniformity and/or discontinuities often occur due to design and manufacturing constraints, thus introducing mode conversion. For example, in a differential-line structure, non-null CM can arise due to asymmetries in the time-domain waveforms (e.g. the in-pair skew due to the presence of a bend), geometry asymmetries in the routing, and/or material asymmetries [43].

A. WIRING STRUCTURES

In wiring structures, mode conversion is introduced by lack of symmetry in the wire arrangement with respect to

[2]Very high frequency LISNs mean the upper working frequency of LISNs is extended from 30 MHz to 300 MHz [38].

ground, such as different conductor heights, dimensions, and/or dielectric coatings. A theoretical investigation of the generation of mode conversion in wiring structure is presented in [44]. Reference [45] provides a statistical investigation of mode conversion in unbalanced cables. Even in the case of balanced cable system, DM-to-CM conversion may still occur due to the connection of branch lines [46].

From the EMC viewpoint cables behave as good antennas. Therefore, when an external EM field couples with a TL, the induced CM noise may be converted into DM noise due to mode conversion. The impact on field-to-wire coupling of coating asymmetry was investigated in [47]. Reference [48] analyzed the generation mechanism of mode conversion in an irregular asymmetrical wire system. A measurement-based statistical model for analyzing CM-to-DM conversion of impulse noise (such as lightning) was introduced in [49]. For suppressing unwanted coupling, twisted wire pairs (TWPs) are commonly used. Although field coupling to TWPs [50] mainly induces CM noise, non-negligible DM noise can be generated by the udesired mode conversion introduced by TWP imbalance [51] and terminal imbalance [50]. Reference [52] investigates mode conversion in automotive cable systems and compares the mode conversion due to unbalanced TWPs and terminals. Another example of noise generation due to CM-to-DM conversion is BCI test, in which if the BCI probe is clamped on a cable harness, CM noise is intentionally injected in the cable system for immunity test. Therefore, CM-to-DM conversion exists in unbalanced system during the BCI test and generates undesired DM noise, which was investigated in [8], [25], and [26], considering cable terminal and wire imbalance, respectively.

B. PCB TRACES

Differential signalling is widely used for high-speed communication. As the signal is transmitted differentially, mode conversion at the PCB level is mainly related to DM-to-CM conversion, and CM disturbances linked to the source are a secondary effect resulting from DM-to-CM conversion. Due to practical design and space constraints on PCBs, imbalanced differential lines are often unavoidable. Reference [53] investigated mode conversion generated by geometric imbalance in differential lines and proposed a general model for analyzing mode conversion in analogy with crosstalk. A time-domain numerical method for CM analysis in inhomogeneous media was provided in [54]. Some extremely imbalanced differential lines were presented and analyzed in [55]. Reference [56] described the mechanism of mode conversion in the differential serpentine delay microstrip line (DSDML) structures, which are widely used for minimizing timing skew in differential signalling, with a special focus on transient CM noise generation. Based on their analysis, the CM noise can be minimized by 1) shorting the parallel trace, 2) making the routing scheme symmetrical, and 3) setting odd section numbers. Mode conversion in DSDMLs can also be significantly suppressed (without degrading differential signals) by adopting embedded coupled lines along the parallel trace sections, as proposed in [57].

Interconnects among different PCBs are the weak points in PCB signal transmission and have to be treated as electrically-large systems starting from the GHz range [58]. Indeed, due to design constraints, these structures may exhibit asymmetries (e.g., in the geometry and materials). Reference [58] analyzed the mode conversion occurring in interconnections due to length mismatch and asymmetrical ground pin configuration, by using transmission line theory. Modal analysis of typical high-speed and high-density connectors can be found in [59], with a specific focus on radiated emissions.

C. LUMPED DISCONTINUITIES

Although mode conversion along transmission lines is usually a distributed phenomenon along the line length, the presence of discontinuities may be interpreted as a lumped source of mode conversion.

In wiring harnesses, a typical example of lumped discontinuities is the interface between two different cables, as investigated in [60] and [61], where the mode conversion occurring at the interface of a 3-wire or 4-wire cable was analyzed.

In PCB traces, bend discontinuities introduce asymmetries, which can be modeled by Π [62] or T [63] lumped circuits. Due to asymmetry, bend discontinuities introduce DM-to-CM conversions. The reason can be attributed to phase skew from the time-domain viewpoint [43], [62], or different inductance and line-to-ground capacitance impedance from the frequency-domain viewpoint [64], [65]. For instance, Fig. 7 shows the T-type equivalent circuit in which the first trace is much longer than the second one and therefore the equivalent components satisfy $L_1 > L_2$ and $C_{1y} > C_{2y}$ [64]. Possible solutions to compensate mode conversion introduced by bend discontinuities include the use of additional capacitors [62], [66], inductors [67], intentionally-asymmetrical traces [64], stepped-impedance traces [68], or specific mushroom structures [69]. Since the main EMC issue is the generation of undesired CM, alternative solutions make use of CM suppression filters. For instance, [70] introduced tightly coupled tapered bends to significantly increase CM impedance without significant impact on DM performance. Another discontinuity in PCB is introduced by vias. In the presence of asymmetrical via configurations, mode conversion occurs. Reference [71] quantified DM-to-CM conversion introduced by different GND via configurations, showing that the difference of the magnitudes of S_{cd21} between worst symmetry and best symmetry can reach 80 dB. Mode conversions due to the combined effect of asymmetrical ground via and TL length mismatch were investigated in [72], which presented the possibility to mitigate mode conversion by properly introducing the two

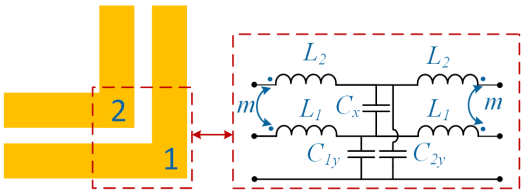

FIGURE 7. *T*-type equivalent circuit of a bend discontinuity.

asymmetrical configurations jointly. Asymmetrical residual via stubs also introduce significant mode conversion, as it has been proved by full-wave simulations [73].

VII. MODE CONVERSION DUE TO OTHER ASYMMETRICAL STRUCTURES

From the EMC analysis viewpoint, it is worth noting that any structure in the system can behave as a noise propagation path although not directly used for the functional EM energy transmission. Several structures, such as mechanical supports, chassis, air-gaps between metallic structures, etc., may introduce asymmetrical paths and cause mode conversion. Reference [74] showed how the imbalance of the parasitic capacitances between different components and the ground can contribute to CM noise generation. In [75], the mode conversion due to parasitic capacitances introduced by asymmetrical busbar was discussed. Those parasitic parameters can be evaluated by measurement [76], [77], analytical formulas [78], or 3D full-wave EM simulation [79]. In order to reduce the CM noise due to parasitic elements, a common method is to balance the corresponding impedances affecting CM noise. For this purpose, some works adjust the impedances to reach the balance condition according to the Wheatstone bridge. This idea has been proved to be effective in several power converter systems, such as boost-converters [74], inverter-based motor drive systems [80], and grid-connected inverters [81].

Additionally, it is noteworthy that even power filters, developed for the purpose of suppressing EMI noise, may potentially introduce mode conversion as a result of unbalanced parameters, thereby leading to undesired noise. A systematic discussion on mode conversion in EMI filters was provided in [82]. In this work, it was also proved that mode conversion due to imbalance of some components makes filters inefficient at certain frequencies. This negative effect can be greatly alleviated by a balanced design of component impedance and layout. For instance, in [83] the imbalance effect linked to the magnetic flux leakage of CM chokes was accurately accounted for in the computation of component impedance. A measurement-based characterization of CM choke in the modal domain was presented in [84]. Mode conversion arising because of unbalanced filter capacitors was investigated in [85], where a capacitor tolerance criterion was introduced to prevent filter degradation. To reduce mode conversion in a filter with unbalanced inductors, [86] proposed to intentionally create a cutout in the ground layer to increase the return-path impedance and demonstrated that this method reduces mode conversion by at least 4 dB in most frequencies, without any additional component.

VIII. CIRCUIT MODELLING OF MODE CONVERSION

As discussed in previous sections, mode conversion due to system asymmetry exists in electrical and electronic systems and plays a crucial role in EMC. Therefore, the development of equivalent circuit models representing mode conversion is of great interest to unveil its physical meaning and its link to system asymmetry. For quantitative estimates of mode conversion, equivalent circuit models can be employed in circuit-based simulations, or in co-simulation with other solvers. To explicitly show the phenomenon of mode conversion, it is common practice to decompose the physical network into DM and CM equivalent circuits, by implementing the modal transformations in Sec. II. The resulting DM and CM equivalent circuits are uncoupled in the absence of mode conversion. Conversely, if mode conversion occurs, they are linked to each other through suitable controlled voltage and current sources. The controlled sources in each modal circuit are proportional to voltages and currents in the other circuit and to suitable electrical/geometrical parameters representative for the asymmetries giving rise to mode conversion. This provides a circuital interpretation of mode conversion, and allows to easily determine the physical parameters responsible for the generation of undesired noise. This is extremely useful for EMC analysis and troubleshooting. Furthermore, mode conversion can be regarded as a "coupling" factor between those equivalent modal circuits, and has a similar effect to the mutual coupling in crosstalk problems. Considering the parallelism between the two phenomena, crosstalk analysis theory can be leveraged to study mode conversion. This section will review the modelling techniques of mode conversion occurring at generation, transmission and reception of EM energy. Finally, its formal analogy to crosstalk will be outlined, and an important assumption to derive decoupled equivalent circuits will be presented. Apart from specific examples, e.g. [8], involving multi-conductor systems, most of the modelling techniques available in the literature were developed for three conductor systems where only one CM and one DM can be introduced. Therefore, without loss of generality, the following discussion will focus on the three conductor systems only.

A. MODELLING OF TERMINAL MODE CONVERSION

Consider the general terminal network, shown in Fig. 8(a), where the impedances Z_g and $Z_{1,2}$ can be frequency dependent. Based on (5) and (11), the corresponding impedance matrix can be written in the modal domain as [46]:

$$\begin{bmatrix} Z_{CM} & Z_{\Delta} \\ Z_{\Delta} & Z_{DM} \end{bmatrix} = \mathbf{T}_{Vm2_2} \begin{bmatrix} Z_1 + Z_g & Z_g \\ Z_g & Z_2 + Z_g \end{bmatrix} \mathbf{T}_{Im2_2}^{-1} = \begin{bmatrix} Z_g + \frac{Z_1+Z_2}{4} & \frac{Z_1-Z_2}{2} \\ \frac{Z_1-Z_2}{2} & Z_1 + Z_2 \end{bmatrix} \tag{34}$$

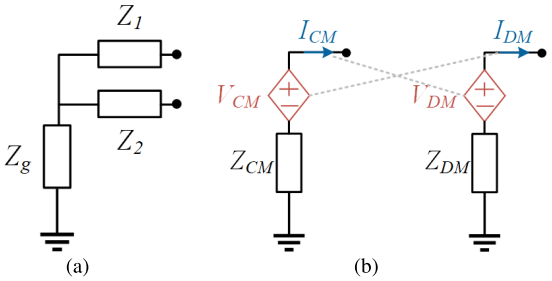

FIGURE 8. (a) Original circuit and (b) mode-conversion model of terminations.

where Z_{CM} and Z_{DM} are the CM and DM impedances, and Z_Δ accounts for mode conversion. If the series impedances Z_1, Z_2 are expressed as function of the differential impedance Z_D by the general expression:

$$Z_{\frac{1}{2}} = Z_D(1 \pm \delta)/2, \, 0 < \delta < 1. \tag{35}$$

(34) can be rewritten as [33]:

$$\begin{bmatrix} Z_{CM} & Z_\Delta \\ Z_\Delta & Z_{DM} \end{bmatrix} = \begin{bmatrix} Z_D/4 + Z_g & \delta Z_D/2 \\ \delta Z_D/2 & Z_D \end{bmatrix}. \tag{36}$$

where δ quantifies the degree of imbalance affecting the terminal network, that is the larger is δ, the larger the mode conversion. From the circuit viewpoint, the effects due to DM-to-CM and CM-to-DM conversion can be included into the equivalent CM and DM circuits, respectively, by the controlled voltage sources in Fig. 8(b) with general expression:

$$V_{CM,DM} = -Z_\Delta I_{DM,CM} \tag{37}$$

where $I_{DM,CM}$ are DM/CM terminal currents.

B. MODELLING OF MODE CONVERSION IN TRANSMISSION LINES

In most applications, cables and PCB lands result to be electrically long and therefore should be analyzed by using MTL theory, [1], [87]. Based on MTL theory, advanced models oriented to mode conversion analysis were proposed by several Authors.

The starting point is to convert into modal quantities the line p.u.l. parameters matrices, which account for electrical and geometrical characteristics of the line cross-section, by using the similarity transformation matrices in Sec. II. For an MTL with N signal conductors, the Telegrapher equtions along x are written as

$$\begin{cases} \dfrac{d}{dx}\boldsymbol{V}(x,\omega) = -j\omega\mathbf{L}_l(x,\omega)\boldsymbol{I}(x,\omega) \\ \dfrac{d}{dx}\boldsymbol{I}(x,\omega) = -j\omega\mathbf{C}_l(x,\omega)\boldsymbol{V}(x,\omega) \end{cases} \tag{38}$$

where $\boldsymbol{V}$ and $\boldsymbol{I}$ are voltage and current $N \times 1$ vectors, $\mathbf{L}_l$ and $\mathbf{C}_l$ are $N \times N$ p.u.l. inductance and capacitance matrices. In the reminder of this work, $\mathbf{L}_l$ and $\mathbf{C}_l$ will be also used to

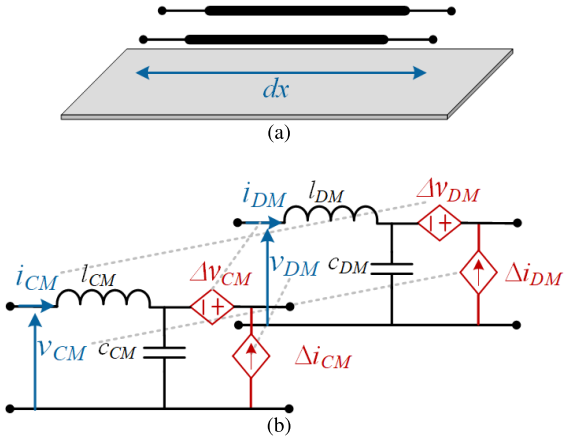

FIGURE 9. (a) Original circuit and (b) CM and DM equivalent circuits of a *dx* section of MTL, with dinstributed sources accounting for mode conversion.

represent the p.u.l. parameters of lossy MTLs, by resorting to the general definitions [12]:

$$\begin{aligned} \mathbf{L}_l(x,\omega) &= \mathbf{l}(x,\omega) + \mathbf{r}(x,\omega)/(j\omega) \\ \mathbf{C}_l(x,\omega) &= \mathbf{c}(x,\omega) + \mathbf{g}(x,\omega)/(j\omega) \end{aligned} \tag{39}$$

where $\mathbf{l}$, $\mathbf{c}$, $\mathbf{r}$, $\mathbf{g}$ are the actual p.u.l. inductance, capacitance, resistance, and conductance matrices, respectively. The dependence on x and ω will be omitted hereafter for brevity.

Similar to (34), the modal inductance and capacitance matrices can be obtained by

$$\begin{aligned} \mathbf{L}_{lM} &= \mathbf{T}_{Vm} \cdot \mathbf{L}_l \cdot \mathbf{T}_{Im}^{-1} \\ \boldsymbol{C}_{lM} &= \mathbf{T}_{Im} \cdot \mathbf{C}_l \cdot \mathbf{T}_{Vm}^{-1} \end{aligned} \tag{40}$$

For a three-conductor TL, (see: Fig. 9(a)), with p.u.l. parameters

$$\mathbf{L}_{l2} = \begin{bmatrix} l_1 & l_m \\ l_m & l_2 \end{bmatrix}; \quad \mathbf{C}_{l2} = \begin{bmatrix} c_1 & c_m \\ c_m & c_2 \end{bmatrix}, \tag{41}$$

where c_m has negative value. The use of the transformation matrices in (11) leads to [53]

$$\begin{aligned} \mathbf{L}_{lM} &= \begin{bmatrix} l_{CM} & \Delta l \\ \Delta l & l_{DM} \end{bmatrix} = \begin{bmatrix} \frac{l_1+l_2+2l_m}{4} & \frac{l_1-l_2}{2} \\ \frac{l_1-l_2}{2} & l_1+l_2-2l_m \end{bmatrix} \\ \boldsymbol{C}_{lM} &= \begin{bmatrix} c_{CM} & \Delta c \\ \Delta c & c_{DM} \end{bmatrix} = \begin{bmatrix} c_1+c_2+2c_m & \frac{c_1-c_2}{2} \\ \frac{c_1-c_2}{2} & \frac{c_1+c_2-2c_m}{4} \end{bmatrix} \end{aligned} \tag{42}$$

where L_{CM}, C_{CM} and L_{DM}, C_{DM} are the CM and DM inductance, capacitance. The out-diagonal entries Δl, Δc account for the non-null mode conversion occurring whenever there are cross-section asymmetries. Accordingly, mode conversion can still be modelled by the use of induced sources in the equivalent DM/CM circuit, as shown in Fig. 9. The difference with respect to the previous case is that these induced sources are *distributed* along the lines, that is:

$$\begin{aligned} \Delta v_{CM,DM} &= -j\omega\Delta l i_{DM,CM} \\ \Delta i_{CM,DM} &= -j\omega\Delta c v_{DM,CM}. \end{aligned} \tag{43}$$

It is worth noting here that line non-uniformity does not necessarily implies mode conversion. For instance,

FIGURE 10. Example of nonuniform structure not introducing mode conversion: symmetrical tapered differential line.

ideal tapered differential lines (see: Fig. 10), whose characteristic impedance gradually varies, exhibit symmetrical cross-section for each x. In this case, Δl, Δc are null and therefore mode conversion does not occur. [44] and [88] provide systematical analyses of mode conversion in asymmetrical nonuniform cables and PCB traces, respectively.

Regarding lumped discontinuities, such as the PCB bend in Fig. 7, the procedure and the equivalent circuits are similar, since a bend can be seen as an electrically-short section of transmission line, where the asymmetry steems from the different length of the two conductors. A circuit model of mode conversion due to bend discontinuities was provided in [64]. Reference [89] showed a TL-based model for computing mode conversion due to asymmetrical via configurations, in terms of mixed-mode S-parameters.

Another modelling technique for lumped discontinuities is to compute the change of current imbalance levels before and after the discontinuity. For this purpose, some works [90], [91] proposed to use the so-called current division factor (or current imbalance factor), h ($0 \leq h \leq 1$), which is the ratio of the CM current flowing in a signal conductor and the total CM current returning through the reference ground [90]:

$$\begin{aligned} I_1 &= hI_{CM} + I_{DM} \\ I_2 &= (1-h)I_{CM} - I_{DM} \end{aligned} \tag{44}$$

where $h = 0.5$ indicates a current-balanced line. Specifically, following this definition, the modal decomposition matrices (based on the relationship defined in (1)) are derived as

$$\mathbf{T}_{Vm2'_2} = \begin{bmatrix} h & 1-h \\ 1 & -1 \end{bmatrix}; \quad \mathbf{T}_{Im2'_2} = \begin{bmatrix} 1 & 1 \\ 1-h & -h \end{bmatrix}. \tag{45}$$

where the current imbalance is represented by h. An extended mixed-mode S-parameters matrix defined based on this definition is shown in [92]. When $h = 0.5$, (45) coincides with the canonical decomposition in (11). It is worth noting that a current-imbalanced line ($h \neq 0.5$) does not necessarily imply mode conversion. In other words, h itself is not a metric for mode conversion. Mode conversion is rather to be ascribed to a variation of h, not to the specific value of this parameter. Therefore, for an interface discontinuity it is computed as the difference between the current division factor before (h_l) and after (h_r) the interface as:

$$\Delta h = h_r - h_l. \tag{46}$$

Then, as presented in Fig. 11, DM-to-CM and CM-to-DM conversions can be modelled by voltage and current sources

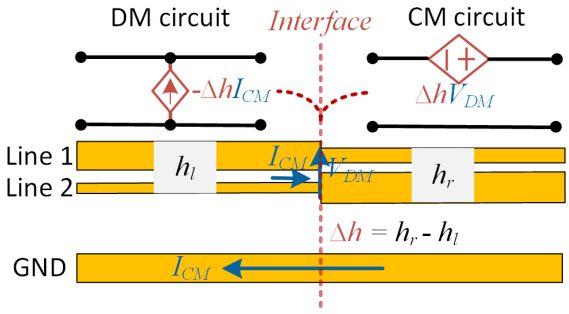

FIGURE 11. Mode-conversion model of a sharp discontinuity.

controlled by the CM current I_{CM} and the DM voltage V_{DM} at the connection interface, through the relations:

$$V_{CM} = \Delta h V_{DM}; \; I_{DM} = -\Delta h I_{CM}. \tag{47}$$

This model proved to be particularly suitable for the analysis of sharp (i.e. ideally zero-length) discontinuities, such as the interface between different cables [60], pigtail connection [61], a PCB board and a cable [93], etc. This method can also be implemented in the study of bend discontinuities [65]. It is worth mentioning that although originally introduced to predict DM-CM quantities in a three-wire system, it also offers the possibility to predict the antenna-mode current,[3] in two-wire systems without ground [94].

C. WEAK-IMBALANCE ASSUMPTION AND ITS ANALOGY TO CROSSTALK

Previous models outline that mode conversion is a bi-directional phenomenon of coupling between modal circuits. In other words, DM-to-CM and CM-to-DM conversions concurrently exist, and should be analyzed simultaneously. However, under specific assumptions, it is possible to uncouple the analysis of the two circuits, which significantly ease their implementation in traditional circuit solvers. This is possible if two conditions are satisfied. First of all, one of the two models should be dominant over the other one. This condition is often satisfied in EMC problems. For instance, if a differential signal is transmitted along a differential line, the DM mode is the dominant mode and the CM mode is ideally null. In a similar fashion, if an electromagnetic field is impinging on the same differential line, a dominant CM noise is induced at the terminations, whereas the DM is ideally null. In the presence of a dominant mode if the imbalance affecting the system is weak, it was proven in [33], [53] that the solution of the two modal

[3] Antenna-mode current is the current whose return paths cannot be evaluated. In other words, the current's return path is located at a ground plane infinitely distant: This definition is incompatible with circuit and MTL theories. Furthermore, the so-called "antenna-mode voltage" along a line is also indefinable since the reference ground is unknown. Therefore, although sometimes antenna-mode current is also named as CM current, it is worth noting that antenna-mode current is different from the general CM/asymmetrical-mode/even-mode current that obeys Kirchhoff's current law at terminals.

TABLE 2. Main- and secondary-modes for mode conversion and crosstalk.

	Main-mode (source) circuit	Secondary-mode (victim) circuit
Crosstalk	Generator conductor	Receptor conductor
DC power supply	DM circuit	CM circuit
Single-phase power supply/signalling		
Three-phases power supply	DM circuits	
Differential signalling	DM circuit	
Field-to-wire coupling	CM circuit	DM circuit(s)
BCI test		

TABLE 3. Circuit models of mode conversion and its analogy to crosstalk. DM-to-CM conversion is shown as an example. CM-to-DM conversion can be obtained in a similar fashion.

	Coupling coefficient	Induced sources	Combinations of inductive and capacitive contributions at terminals
Crosstalk	Mutual inductance (l_m) Mutual capacitance (c_m) ($c_m < 0$)	Inductive coupling: $\Delta V = -j\omega l_m I_g$ Capacitive coupling: $\Delta I = -j\omega c_m V_g$	Left: Sum; Right: Subtraction
Mode conversion			
Terminal imbalance	Difference of line series impedances (Z_Δ)	$V_{CM} = -Z_\Delta I_{DM}$	N.A.
Line imbalance	Cross-modes of p.u.l. parameters ($\Delta l(x)$,$\Delta c(x)$)	$\Delta V_{CM}(x) = -j\omega\Delta l(x)\, I_{DM}(x)$ $\Delta I_{CM}(x) = -j\omega\Delta c(x)\, V_{DM}(x)$	Left: Sum; Right: Subtraction
PCB bend	Cross-modes of (equivalent) lumped parameters (Δl,Δc)	$\Delta V_{CM} = -j\omega\Delta l\, I_{DM}$ $\Delta I_{CM} = -j\omega\Delta c\, V_{DM}$	Left: Subtraction; Right: Sum
Unequal components in filters and LISNs			Depending on component values

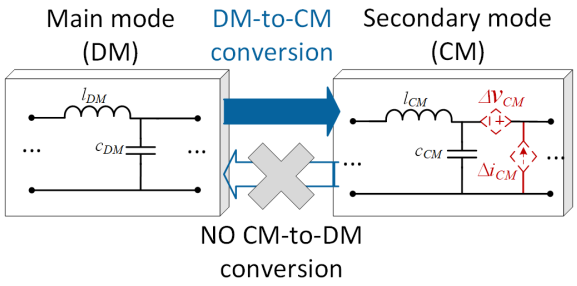

FIGURE 12. Example of interactions between modal circuits under the assumption of weak imbalance (here the DM mode is the dominant one).

circuits can be uncoupled. Accordingly, the dominant-mode circuit can be solved as the first step, by neglecting the back interaction from the secondary one. Once voltages and currents on the dominant circuit are known, they become input data for subsequent solution of the secondary circuit(s). A principle drawing is shown in Fig. 12, where the DM mode is the dominant mode and the CM is the secondary mode. The solution encompasses the following three steps [95]: 1) the DM circuit is solved independently, neglecting the interaction with the CM circuit; 2) In the CM circuit, DM-to-CM conversion is modelled by induced sources controlled by the obtained DM quantities; 3) The obtained CM circuit is eventually solved. This unidirectional process is similar to crosstalk analysis [2] under the weak-coupling assumption, where the back interaction from the receptor circuit to the generator circuit is neglected [96]. In crosstalk, the generator and receptor circuits are coupled through mutual inductances (l_m) and capacitances (c_m). If mutual coupling is weak, it is possible to ignore the influence of the voltages/currents induced in the receptor circuit on the generator [2]. In a similar fashion, here, DM and CM circuits are coupled through inductive (Δl) and capacitive (Δc) imbalance coefficients. If the imbalance is weak, it is possible to ignore the influence of the voltages and currents induced in the secondary circuit (i.e., the CM circuit in Fig. 12) on the main modal circuits (i.e., in Fig. 12 the DM circuit).

Empirical conditions for weak imbalance were formulated in [33] and [53]. As far as terminal imbalance is concerned, if the imbalance coefficient δ in (36) is lower or equal to 0.4, the CM-to-DM back-interaction can be neglected. For line imbalance, the coupling coefficients:

$$k_l = \frac{\Delta L}{\sqrt{L_{CM} L_{DM}}}; \quad k_c = \frac{\Delta C}{\sqrt{C_{CM} C_{DM}}} \tag{48}$$

were introduced. As a rule of thumb, MTL geometrical imbalance is considered to be weak if the condition $\max({k_l}^2, {k_c}^2) < 0.1$ is satisfied. A Spice-based circuit model involving both terminal and line imbalances was presented in [97]. Reference [95] demonstrated that this assumption can be combined with other MTL methods to improve computational efficiency. Reference [98] used

this assumption for the development of MTL model for high-speed cable systems. Reference [75] analyzed the mode conversion due to unbalanced busbar of a converter system.

A practical example in which the CM is the dominant mode is represented by BCI test setups for conducted susceptibility verification. Indeed, as long as a BCI probe is clamped on a wire bundle, only CM noise is theoretically injected. However, due to asymmetries in the system under test, also a non-null DM noise usually stresses the system terminations, possibly giving rise to immunity issues. To predict such DM noise, it is possible to neglect the back-interaction of the DM on the CM. Under this assumption, [8] shows that accurate prediction of line voltages can be obtained by solving a one conductor CM equivalent circuit as the first step and by subsequentially evaluating the DM voltages through CM-to-DM conversion.

The analogy with crosstalk allows the interpretation of mode conversion as superposition of ''inductive'' and ''capacitive'' contributions. In crosstalk, since the mutual capacitance c_m has negative value, inductive and capacitive contributions sum at the left terminal and subtract at the right terminal [2]. Similarly, in line imbalance, if the inductive coefficient Δl is positive, the capacitive coefficient Δc is negative and vice-versa. Hence, inductive and capacitive contributions at the line terminals combine as in crosstalk. This is no longer true as far as mode conversion due to bend discontinuities is considered [64]. Indeed, in this case, the longer trace (Trace #1 in Fig. 7) exhibits both larger self-inductance and capacitance. Therefore, Δl and Δc have the same sign, resulting in a different superposition of inductive and capacitive contributions at the terminals.

IX. CONCLUSION

Avoiding mode conversion is one of the main challenges for EMC design and diagnosis. A comprehensive review of EMC-oriented mode conversion and modal analysis was presented in this paper. Mode decompositions and metrics for mode conversion in the literature were summarized and analyzed. An overview of mode conversion in electronic and electrical systems was given and the main contributions investigating common structures in which mode conversion can potentially occur were reviewed in detail. Any implicit and/or explicit asymmetry affecting the structure is the fundamental step for the investigation of mode conversion. Circuit modelling techniques and the weak-imbalance assumption were discussed and the strict analogy between mode conversion and crosstalk was outlined. A summary of the available prediction models is presented in Tab. 2 and 3. This review provided thorough information for detecting, analyzing, and modelling mode conversion.

REFERENCES

[1] C. R. Paul, *Analysis of Multiconductor Transmission Lines*. Hoboken, NJ, USA: Wiley, 2008.
[2] C. R. Paul, *Introduction to Electromagnetic Compatibility*. Hoboken, NJ, USA: Wiley, 2006.
[3] G. I. Zysman and A. K. Johnson, ''Coupled transmission line networks in an inhomogeneous dielectric medium,'' *IEEE Trans. Microw. Theory Techn.*, vol. MTT-17, no. 10, pp. 753–759, Oct. 1969.
[4] D. E. Bockelman and W. R. Eisenstadt, ''Combined differential and common-mode scattering parameters: Theory and simulation,'' *IEEE Trans. Microw. Theory Techn.*, vol. 43, no. 7, pp. 1530–1539, Jul. 1995.
[5] S. Wang, F. Luo, and F. C. Lee, ''Characterization and design of three-phase EMI noise separators for three-phase power electronics systems,'' *IEEE Trans. Power Electron.*, vol. 26, no. 9, pp. 2426–2438, Sep. 2011.
[6] J. L. Blackburn, *Symmetrical Components for Power Systems Engineering*. Boca Raton, FL, USA: CRC Press, 2017.
[7] J. Jia, D. Rinas, and S. Frei, ''Predicting the radiated emissions of automotive systems according to CISPR 25 using current scan methods,'' *IEEE Trans. Electromagn. Compat.*, vol. 58, no. 2, pp. 409–418, Apr. 2016.
[8] N. Toscani, X. Wu, D. Spina, D. V. Ginste, and F. Grassi, ''A two-step approach for the analysis of bulk current injection setups involving multiwire bundles,'' *IEEE Trans. Electromagn. Compat.*, vol. 65, no. 1, pp. 126–137, Feb. 2023.
[9] G. Andrieu, L. Kone, F. Bocquet, B. Demoulin, and J. P. Parmantier, ''Multiconductor reduction technique for modeling common-mode currents on cable bundles at high frequency for automotive applications,'' *IEEE Trans. Electromagn. Compat.*, vol. 50, no. 1, pp. 175–184, 2008.
[10] J. Wang, X. Song, D. Su, and B. Li, ''Near-field radiation calculation of irregular wiring twisted-wire pairs based on mode decomposition,'' *IEEE Trans. Electromagn. Compat.*, vol. 59, no. 2, pp. 600–608, Apr. 2017.
[11] A. Ferrero and M. Pirola, ''Generalized mixed-mode S-parameters,'' *IEEE Trans. Microw. Theory Techn.*, vol. 54, no. 1, pp. 458–463, Jan. 2006.
[12] X. Wu, P. Manfredi, D. Vande Ginste, and F. Grassi, ''A hybrid perturbative-stochastic Galerkin method for the variability analysis of nonuniform transmission lines,'' *IEEE Trans. Electromagn. Compat.*, vol. 62, no. 3, pp. 746–754, Jun. 2020.
[13] Y. X. Teo, A. R. Ruddle, and J. Chen, ''Comparison of unshielded twisted pair and flexible printed circuit interconnects for data networks,'' in *Proc. Int. Symp. Electromagn. Compat.*, Aug. 2018, pp. 96–101.
[14] F. Grassi, L. Badini, G. Spadacini, and S. A. Pignari, ''Crosstalk and mode conversion in adjacent differential lines,'' *IEEE Trans. Electromagn. Compat.*, vol. 58, no. 3, pp. 877–886, Jun. 2016.
[15] D. E. Bockelman and W. R. Eisenstadt, ''Pure-mode network analyzer for on-wafer measurements of mixed-mode S-parameters of differential circuits,'' *IEEE Trans. Microw. Theory Techn.*, vol. 45, no. 7, pp. 1071–1077, Jul. 1997.
[16] W. Fan, A. Lu, L. L. Wai, and B. K. Lok, ''Mixed-mode S-parameter characterization of differential structures,'' in *Proc. 5th Electron. Packag. Technol. Conf. (EPTC)*, 2003, pp. 533–537.
[17] *Transmission Aspects of Unbalance About Earth*, Int. Telecommun. Union, document ITU-T Recommendation G. 117, 1996.
[18] *Measuring Arrangements to Assess the Degree of Unbalance About Earth*, Int. Telecommun. Union, document ITU-T Recommendation O. 9, 1999.
[19] T. Matsushima, A. Sugiura, and O. Wada, ''Differential-/common-mode conversion loss and LCL/TCL measurement methods,'' *IEEE Trans. Electromagn. Compat.*, vol. 62, no. 5, pp. 1830–1839, Oct. 2020.
[20] *Method for Measuring Longitudinal Conversion Loss (9 KHZ-30 MHZ)*, Int. Telecommun. Union, document ITU-T Recommendation K. 86, 2011.
[21] *Multicore and Symmetrical Pair/Quad Cables for Digital Communications: Part 1–2: Electrical Transmission Characteristics and Test Methods of Symmetrical Pair/Quad Cables*, Int. Electrotechnical Commission, Standard IEC TS 61156-1-2, 2023.
[22] *IEEE Standard for Ethernet*, IEEE Standard 802.3-2022, 2022.
[23] *Information Technology—Generic Cabling for Customer Premises—Part 1: General Requirements*, Int. Electrotechnical Commission, Standard ISO/IEC 11801-1, Nov. 2017.
[24] S. Wang, F. C. Lee, and W. G. Odendaal, ''Characterization, evaluation, and design of noise separator for conducted EMI noise diagnosis,'' *IEEE Trans. Power Electron.*, vol. 20, no. 4, pp. 974–982, Jul. 2005.
[25] F. Grassi and S. A. Pignari, ''Bulk current injection in twisted wire pairs with not perfectly balanced terminations,'' *IEEE Trans. Electromagn. Compat.*, vol. 55, no. 6, pp. 1293–1301, Dec. 2013.
[26] S. Rasm, G. Andrieu, A. Reineix, and R. Tumayan, '''Virtual' signal integrity test on shielded/unshielded twisted-wire pairs using the bulk current injection setup,'' *IEEE Trans. Electromagn. Compat.*, vol. 63, no. 5, pp. 1357–1365, Oct. 2021.

[27] H. W. Ott and H. W. Ott, *Noise Reduction Techniques in Electronic Systems*, vol. 442. New York, NY, USA: Wiley, 1988.

[28] H. Rezaei, M. Sørensen, W. Huang, D. G. Beetner, and D. Pommerenke, "Analyzing the influence of imbalanced two-or three-wire VHF LISN on radiated emissions from AC cables," *IEEE Trans. Electromagn. Compat.*, vol. 64, no. 2, pp. 327–337, Apr. 2022.

[29] P. S. Niklaus, M. M. Antivachis, D. Bortis, and J. W. Kolar, "Analysis of the influence of measurement circuit asymmetries on three-phase CM/DM conducted EMI separation," *IEEE Trans. Power Electron.*, vol. 36, no. 4, pp. 4066–4080, Apr. 2021.

[30] M. Perotti and F. Fiori, "Evaluation of the common mode and the differential mode components from conducted emission measurements," *IEEE Trans. Electromagn. Compat.*, vol. 64, no. 3, pp. 884–892, Jun. 2022.

[31] P. Wu, Z. Xu, Z. Xu, Y. Jiang, C. Meng, and J. Fan, "Kron's model for the radiated immunity and signal integrity analysis of multi-conductor shielded cable," *IEEE Trans. Electromagn. Compat.*, vol. 63, no. 6, pp. 2093–2104, Dec. 2021.

[32] D. M. Lauder and R. C. Marshall, "Measurement uncertainty and cable balance-with implications for the CDNE-M and CMAD," in *Proc. Int. Symp. Electromagn. Compat.*, Sep. 2014, pp. 801–806.

[33] F. Grassi, G. Spadacini, and S. A. Pignari, "The concept of weak imbalance and its role in the emissions and immunity of differential lines," *IEEE Trans. Electromagn. Compat.*, vol. 55, no. 6, pp. 1346–1349, Dec. 2013.

[34] F. Grassi and S. A. Pignari, "Immunity to conducted noise of data transmission along DC power lines involving twisted-wire pairs above ground," *IEEE Trans. Electromagn. Compat.*, vol. 55, no. 1, pp. 195–207, Feb. 2013.

[35] S. Okuyama, N. Kuwabara, K. Osabe, and H. Muramatsu, "Improvement of radiated emission measurement reproducibility with VHF-LISN obtained from final results of international inter-laboratory comparison on termination control of power line," in *Proc. Asia–Pacific Symp. Electromagn. Compat. (APEMC)*, May 2015, pp. 589–592.

[36] J. Medler, "Reducing the standard compliance uncertainty by using ferrite type CMADs during radiated disturbance measurements acc. to CISPR 16–2–3," in *Proc. Int. Symp. Electromagn. Compat.*, May 2014, pp. 247–250.

[37] S. Caniggia and C. F. M. Carobbi, "Improving the reproducibility of radiated emission and immunity tests through the use of the CMAD," *IEEE Trans. Electromagn. Compat.*, vol. 61, no. 4, pp. 1370–1376, Aug. 2019.

[38] C. Miyazaki, K. Tanakajima, M. Yamaguchi, K. Endo, H. Muramatsu, and J. Kawano, "A round-robin test on effectiveness of a VHF LISN for radiated emission measurements," in *Proc. IEEE Int. Symp. Electromagn. Compat.*, Aug. 2011, pp. 405–410.

[39] S. Okuyama, K. Osabe, K. Tanakajima, and H. Muramatsu, "Investigation on effectiveness of very high frequency line impedance stabilization network (VHF-LISN) for measurement reproducibility," in *Proc. Int. Symp. Electromagn. Compat.*, Sep. 2013, pp. 174–179.

[40] S. Okuyama, K. Osabe, N. Kuwabara, F. Amemiya, T. Shimasaki, and H. Muramatsu, "Investigating power line termination device effectiveness in regards to radiated emission measurement reproducibility in consideration of two disturbance sources and AC mains cable," in *Proc. Int. Symp. Electromagn. Compat.*, Sep. 2020, pp. 1–6.

[41] K. Osabe, S. Okuyama, N. Kuwabara, and H. Muramatsu, "Consideration to terminating condition of mains cable for radiated emission measurement caused by different disturbance sources," *IEEE Trans. Electromagn. Compat.*, vol. 62, no. 4, pp. 1451–1458, Aug. 2020.

[42] *Vehicles, Boats and Internal Combustion Engines—Radio Disturbance Characteristics—Limits and Methods of Measurement for the Protection of on-Board Receivers*, Int. Electrotechnical Commission, CISPR 25, Geneva, Switzerland, 2021.

[43] B. Archambeault, J. C. Diepenbrock, and S. Connor, "Emi emissions from mismatches in high speed differential signal traces and cables," in *Proc. IEEE Int. Symp. Electromagn. Compat.*, 2007, pp. 1–6.

[44] F. Grassi, P. Manfredi, X. Liu, J. Sun, X. Wu, D. V. Ginste, and S. A. Pignari, "Effects of undesired asymmetries and nonuniformities in differential lines," *IEEE Trans. Electromagn. Compat.*, vol. 59, no. 5, pp. 1613–1624, Oct. 2017.

[45] X. Wu, Y. Yang, F. Grassi, G. Spadacini, and S. A. Pignari, "Statistical characterization of line-imbalance in differential lines," in *Proc. 31th URSI Gen. Assem. Scientific Symp. (URSI GASS)*, Aug. 2014, pp. 1–4.

[46] A. Sugiura and Y. Kami, "Generation and propagation of common-mode currents in a balanced two-conductor line," *IEEE Trans. Electromagn. Compat.*, vol. 54, no. 2, pp. 466–473, Apr. 2012.

[47] B. Li, D. Su, J. Wang, and X. Song, "Common- and differential-mode conversion induced by asymmetry and dielectric coating in a transmission line system," *IEEE Trans. Electromagn. Compat.*, vol. 59, no. 3, pp. 988–991, Jun. 2017.

[48] J. Yang, X. Sun, Y. Zhao, J. Chen, and T. Sun, "Modal response analysis of non-uniform and asymmetric DL under plane-wave illumination," *IET Sci., Meas. Technol.*, vol. 13, no. 4, pp. 553–562, Jun. 2019.

[49] C. Chrysanthou, "Statistical models for differential-mode conversion of common-mode impulse voltages measured on telecommunication pairs," *IEEE Trans. Electromagn. Compat.*, vol. 38, no. 3, pp. 489–495, Aug. 1996.

[50] G. Spadacini, F. Grassi, and S. A. Pignari, "Field-to-wire coupling model for the common mode in random bundles of twisted-wire pairs," *IEEE Trans. Electromagn. Compat.*, vol. 57, no. 5, pp. 1246–1254, Oct. 2015.

[51] Z. Zhou and B. Li, "Modeling mode conversion effects in imbalanced twisted-wire pairs above ground plane," in *Proc. Int. Conf. Microw. Millim. Wave Technol. (ICMMT)*, Sep. 2020, pp. 1–3.

[52] C. Austermann and S. Frei, "Analysis on common to differential mode conversion within automotive communication systems," in *Proc. IEEE Int. Joint EMC/SI/PI EMC Eur. Symp.*, Jul. 2021, pp. 180–185.

[53] F. Grassi, Y. Yang, X. Wu, G. Spadacini, and S. A. Pignari, "On mode conversion in geometrically unbalanced differential lines and its analogy with crosstalk," *IEEE Trans. Electromagn. Compat.*, vol. 57, no. 2, pp. 283–291, Apr. 2015.

[54] S. Jinno, S. Kitora, H. Toki, and M. Abe, "A time-domain three-dimensional numerical method for comprehensive common-mode analysis of electric circuits in inhomogeneous media," *IEEE Trans. Electromagn. Compat.*, vol. 64, no. 6, pp. 2189–2197, Dec. 2022.

[55] Y. Kayano, Y. Tsuda, and H. Inoue, "Identifying EM radiation from asymmetrical differential-paired lines with equi-distance routing," in *Proc. IEEE Int. Symp. Electromagn. Compat.*, Pittsburgh, PA, USA, Aug. 2012, pp. 311–316.

[56] G.-H. Shiue, J.-H. Shiu, Y.-C. Tsai, and C.-M. Hsu, "Analysis of common-mode noise for weakly coupled differential serpentine delay microstrip line in high-speed digital circuits," *IEEE Trans. Electromagn. Compat.*, vol. 54, no. 3, pp. 655–666, Jun. 2012.

[57] S. Lee, J. Lim, S. Oh, and J. Lee, "Common-mode conversion noise mitigation with embedded coupled lines in differential serpentine delay microstrip lines," *IEEE Trans. Electromagn. Compat.*, vol. 62, no. 6, pp. 2558–2566, Dec. 2020.

[58] X. Duan, B. Archambeault, H.-D. Bruens, and C. Schuster, "EM emission of differential signals across connected printed circuit boards in the GHz range," in *Proc. IEEE Int. Symp. Electromagn. Compat.*, Aug. 2009, pp. 50–55.

[59] H.-C. Chen, S. Connor, M. S. Halligan, X. Tian, X. Li, B. Archambeault, J. L. Drewniak, and T.-L. Wu, "Investigation of the radiated emissions from high-speed/high-density connectors," *IEEE Trans. Electromagn. Compat.*, vol. 58, no. 1, pp. 220–230, Feb. 2016.

[60] Y. Toyota, K. Iokibe, and L. R. Koga, "Mode conversion caused by discontinuity in transmission line: From viewpoint of imbalance factor and modal characteristic impedance," in *Proc. IEEE Electr. Design Adv. Packag. Syst. Symp. (EDAPS)*, Dec. 2013, pp. 52–55.

[61] T. Nobunaga, Y. Toyota, K. Iokibe, L. R. Koga, and T. Watanabe, "Evaluation of pigtail termination of STP cable using modal equivalent circuit of four-conductor transmission systems," in *Proc. Int. Symp. Electromagn. Theory*, May 2013, pp. 222–225.

[62] G.-H. Shiue, W.-D. Guo, C.-M. Lin, and R.-B. Wu, "Noise reduction using compensation capacitance for bend discontinuities of differential transmission lines," *IEEE Trans. Adv. Packag.*, vol. 29, no. 3, pp. 560–569, Aug. 2006.

[63] P. H. Harms and R. Mittra, "Equivalent circuits for multiconductor microstrip bend discontinuities," *IEEE Trans. Microw. Theory Techn.*, vol. 41, no. 1, pp. 62–69, Jan. 1993.

[64] X. Wu, F. Grassi, P. Manfredi, D. V. Ginste, and S. A. Pignari, "Compensating mode conversion due to bend discontinuities through intentional trace asymmetry," *IEEE Trans. Electromagn. Compat.*, vol. 62, no. 2, pp. 617–621, Apr. 2020.

[65] Y. Toyota, S. Kan, and K. Iokibe, "Modal equivalent circuit of bend discontinuity in differential transmission lines," in *Proc. Int. Symp. Electromagn. Compat.*, May 2014, pp. 117–120.

[66] B.-R. Huang, C.-H. Chang, R.-Y. Fang, and C.-L. Wang, "Common-mode noise reduction using asymmetric coupled line with SMD capacitor," *IEEE Trans. Compon., Packag., Manuf. Technol.*, vol. 4, no. 6, pp. 1082–1089, Jun. 2014.

[67] C.-H. Chang, R.-Y. Fang, and C.-L. Wang, "Bended differential transmission line using compensation inductance for common-mode noise suppression," *IEEE Trans. Compon., Packag., Manuf. Technol.*, vol. 2, no. 9, pp. 1518–1525, Sep. 2012.
[68] D.-B. Lin, C.-P. Huang, and H.-N. Ke, "Using stepped-impedance lines for common-mode noise reduction on bended coupled transmission lines," *IEEE Trans. Compon., Packag., Manuf. Technol.*, vol. 6, no. 5, pp. 757–766, May 2016.
[69] S. Lee, J. Lim, S. Oh, Y. Kim, D. Oh, and J. Lee, "Differential-to-common-mode conversion suppression using mushroom structure on bent differential transmission lines," *IEEE Trans. Compon., Packag., Manuf. Technol.*, vol. 9, no. 4, pp. 702–711, Apr. 2019.
[70] C. Gazda, D. Vande Ginste, H. Rogier, R.-B. Wu, and D. De Zutter, "A wideband common-mode suppression filter for bend discontinuities in differential signaling using tightly coupled microstrips," *IEEE Trans. Adv. Packag.*, vol. 33, no. 4, pp. 969–978, Nov. 2010.
[71] A. Jaze, B. Archambeault, and S. Connor, "Differential mode to common mode conversion on differential signal vias due to asymmetric GND via configurations," in *Proc. IEEE Int. Symp. Electromagn. Compat.*, Aug. 2013, pp. 735–740.
[72] R. Rimolo-Donadio, X. Duan, H.-D. Bruns, and C. Schuster, "Differential to common mode conversion due to asymmetric ground via configurations," in *Proc. IEEE Workshop Signal Propag. Interconnects*, May 2009, pp. 1–4.
[73] J. Cedeño-Chaves, K. Scharff, A. Carmona-Cruz, H.-D. Brüns, R. Rimolo-Donadio, and C. Schuster, "Mode conversion due to residual via stubs in differential signaling," in *Proc. IEEE 23rd Workshop Signal Power Integr. (SPI)*, Jun. 2019, pp. 1–4.
[74] S. Wang, P. Kong, and F. C. Lee, "Common mode noise reduction for boost converters using general balance technique," *IEEE Trans. Power Electron.*, vol. 22, no. 4, pp. 1410–1416, Jul. 2007.
[75] S. Negri, X. Wu, X. Liu, F. Grassi, G. Spadacini, and S. A. Pignari, "Mode conversion in DC–DC converters with unbalanced busbars," in *Proc. Joint Int. Symp. Electromagn. Compat., Sapporo Asia–Pacific Int. Symp. Electromagn. Compat. (EMC Sapporo/APEMC)*, Jun. 2019, pp. 1–4.
[76] L. Yang and W. G. H. Odendaal, "Measurement-based method to characterize parasitic parameters of the integrated power electronics modules," *IEEE Trans. Power Electron.*, vol. 22, no. 1, pp. 54–62, Jan. 2007.
[77] A. Cataliotti, D. D. Cara, G. Marsala, A. Pecoraro, A. Ragusa, and G. Tinè, "High-frequency experimental characterization and modeling of six pack IGBTs power modules," *IEEE Trans. Ind. Electron.*, vol. 63, no. 11, pp. 6664–6673, Nov. 2016.
[78] G. Grandi, D. Casadei, and U. Reggiani, "Common- and differential-mode HF current components in AC motors supplied by voltage source inverters," *IEEE Trans. Power Electron.*, vol. 19, no. 1, pp. 16–24, Jan. 2004.
[79] J. Oliveira, H. Morel, D. Planson, and F. Loiselay, "Analysis of parasitic elements in power modules based on GaN components," in *Proc. Int. Exhib. Conf. Power Electron., Intell. Motion, Renew. Energy Energy Manag.*, Jul. 2020, pp. 1–6.
[80] L. Xing and J. Sun, "Conducted common-mode EMI reduction by impedance balancing," *IEEE Trans. Power Electron.*, vol. 27, no. 3, pp. 1084–1089, Mar. 2012.
[81] H. Zhang, L. Yang, S. Wang, and J. Puukko, "Common-mode EMI noise modeling and reduction with balance technique for three-level neutral point clamped topology," *IEEE Trans. Ind. Electron.*, vol. 64, no. 9, pp. 7563–7573, Sep. 2017.
[82] S. Wang and F. C. Lee, "Investigation of the transformation between differential-mode and common-mode noises in an EMI filter due to unbalance," *IEEE Trans. Electromagn. Compat.*, vol. 52, no. 3, pp. 578–587, Aug. 2010.
[83] M. Kamikura, Y. Murata, and A. Nishizawa, "Investigation on the mode conversion between common-mode and differential-mode noises in EMI filters for power electronics circuits," in *Proc. Int. Symp. Electromagn. Compat.*, Sep. 2013, pp. 557–560.
[84] Z. Li, D. Pommerenke, and Y. Shimoshio, "Common-mode and differential-mode analysis of common-mode chokes," in *Proc. IEEE Symp. Electromagn. Compatibility. Symp. Rec.*, Aug. 2003, pp. 384–387.
[85] F. Zheng, A. Wang, Z. Wu, T. Gao, Z. Wang, and X. Zhao, "Capacitor tolerance criterion for three-phase EMI filters to attenuate noise of PWM inverters," *IEEE Trans. Power Electron.*, vol. 36, no. 8, pp. 9080–9092, Aug. 2021.
[86] S. Penugonda, Z. Xu, Y. Guo, M. Ouyang, M. Kim, J. Lee, J. Ha, H. Lee, S. Yun, J. Fan, and H. Kim, "Reduction of mode conversion of differential-mode noise to common-mode noise by printed circuit board modification for unbalanced EMI filter network," in *Proc. IEEE Int. Joint EMC/SI/PI EMC Eur. Symp.*, Jul. 2021, pp. 261–264.
[87] G. Antonini, A. Orlandi, and S. A. Pignari, "Review of Clayton R. Paul studies on multiconductor transmission lines," *IEEE Trans. Electromagn. Compat.*, vol. 55, no. 4, pp. 639–647, Aug. 2013.
[88] X. Wu, F. Grassi, X. Liu, J. Sun, S. A. Pignari, P. Manfredi, and D. V. Ginste, "Generation of common mode in non-uniform differential interconnections," in *Proc. Asia–Pacific Int. Symp. Electromagn. Compat. (APEMC)*, Jun. 2017, pp. 256–258.
[89] S. Pan and J. Fan, "Equivalent mixed-mode characteristic impedances for differential signal vias," in *Proc. IEEE Int. Symp. Electromagn. Compat.*, Aug. 2009, pp. 74–79.
[90] T. Watanabe, O. Wada, T. Miyashita, and R. Koga, "Common-mode current generation caused by difference of unbalance of transmission lines on a printed circuit board with narrow ground pattern," *IEICE Trans. Commun.*, no. 3, pp. 593–599, Mar. 2000.
[91] K. Sejima, Y. Toyota, K. Iokibe, L. R. Koga, and T. Watanabe, "Experimental model validation of mode-conversion sources introduced to modal equivalent circuit," in *Proc. IEEE Int. Symp. Electromagn. Compat.*, Aug. 2012, pp. 492–497.
[92] N. Zhang, K. Kim, H. Lee, and W. Nah, "Theory, simulation, and experiment on extended mixed-mode S-parameters in three-conductor lines," *IEEE Trans. Electromagn. Compat.*, vol. 59, no. 6, pp. 1932–1939, Dec. 2017.
[93] M. A. Islam, M. Himuro, K. Iokibe, and Y. Toyota, "Common-mode current reduction by applying mode-conversion suppression technique to power delivery network as side-channel attack countermeasure," in *Proc. Int. Conf. Comput., Commun., Chem., Mater. Electron. Eng. (IC4ME)*, Dec. 2021, pp. 1–4.
[94] L. Niu and T. H. Hubing, "Rigorous derivation of imbalance difference theory for modeling radiated emission problems," *IEEE Trans. Electromagn. Compat.*, vol. 57, no. 5, pp. 1021–1026, Oct. 2015.
[95] X. Wu, F. Grassi, P. Manfredi, and D. V. Ginste, "Perturbative analysis of differential-to-common mode conversion in asymmetric nonuniform interconnects," *IEEE Trans. Electromagn. Compat.*, vol. 60, no. 1, pp. 7–15, Feb. 2018.
[96] C. R. Paul, "Solution of the transmission-line equations under the weak-coupling assumption," *IEEE Trans. Electromagn. Compat.*, vol. 44, no. 3, pp. 413–423, Aug. 2002.
[97] F. Grassi, X. Wu, Y. Yang, G. Spadacini, and S. A. Pignari, "Modeling of imbalance in differential lines targeted to spice simulation," *Prog. Electromagn. Res. B*, vol. 62, pp. 225–239, 2015.
[98] O. Gassab, Y. Chen, Y. Shao, J. Li, D.-E. Wen, F. He, Z. Su, P. Zhong, J. Wang, D. Zhao, and W.-Y. Yin, "Accurate formulation of the skin and proximity effects in high-speed cable system," *IEEE Access*, vol. 10, pp. 100682–100699, 2022.

LUDOVICA ILLIANO received the M.Sc. degree (cum laude) in electrical engineering from Politecnico di Milano, Milan, Italy, in 2020, where she is currently pursuing the Ph.D. degree in electrical engineering with the Department of Electronics, Information, and Bioengineering. From 2020 to 2021, she was a Hardware Engineer with Thales Alenia Space, Milan. Her research interests include mode conversion analysis, communication systems, automotive EMC issues, and components modeling for SI and EMC analysis purposes.

XINGLONG WU (Senior Member, IEEE) received the double M.Sc. degrees from Xi'an Jiaotong University, Xi'an, China, and Politecnico di Milano, Milan, Italy, in 2015, and the Ph.D. degree (cum laude) from Politecnico di Milano, in 2019, all in electrical engineering.

He is currently an Assistant Professor with the Department of Electronics, Information and Bioengineering, Politecnico di Milano. In March 2017 and June 2017, he was a Visiting Scientist with the Electromagnetics Group, Department of Information Technology, Ghent University, Belgium. From 2019 to 2020, he was a Postdoctoral Research Fellow with Politecnico di Milano. His research interests include distributed parameter circuit modeling, statistical techniques for electromagnetic compatibility (EMC), experimental procedures and setups for EMC testing, power electronics EMC, and system-level EMC.

Dr. Wu was the recipient of the International Union of Radio Science (URSI) Young Scientist Award from the 2020 URSI General Assembly and Scientific Symposium.

FLAVIA GRASSI (Senior Member, IEEE) received the Laurea (M.Sc.) and Ph.D. degrees in electrical engineering from Politecnico di Milano, Milan, Italy, in 2002 and 2006, respectively.

From 2008 to 2009, she was with European Space Agency (ESA), ESA/ESTEC, The Netherlands, as a Research Fellow. She is currently a Full Professor with the Department of Electronics, Information and Bioengineering, Politecnico di Milano. Her research interests include theoretical and experimental characterization of EM interference via lumped and distributed circuit modeling; characterization and development of measurement procedures and setups for EMC assessment of avionic, automotive, and power systems; and statistical techniques, EMC, and coexistence issues in power systems. She received the International Union of Radio Science (URSI) Young Scientist Award, in 2008, and the IEEE Young Scientist Award from the 2016 Asia-Pacific International Symposium on EMC (APEMC), the IEEE EMC Society 2016 and 2021 Transactions Prize Paper Award, and the Best Symposium Paper Award at the 2015 and 2018 APEMC.

GIORDANO SPADACINI (Senior Member, IEEE) received the Laurea (M.Sc.) and Ph.D. degrees in electrical engineering from Politecnico di Milano, Italy, in 2001 and 2005, respectively.

He is currently an Associate Professor with the Department of Electronics, Information and Bioengineering, Politecnico di Milano. His research interests include statistical models for the characterization of interference effects, distributed parameter circuit modeling, experimental procedures and setups for EMC testing, and EMC in aerospace, automotive, and railway systems. He was a co-recipient of the 2005 EMC Transactions Prize Paper Award, the 2016 and 2021 R. B. Schulz Best EMC Transactions Paper Award, two Best Symposium Paper Awards from the 2015 Asia-Pacific International Symposium on EMC (APEMC), and the 2018 Joint IEEE EMC and APEMC Symposium.

SERGIO A. PIGNARI (Fellow, IEEE) received the Laurea (M.Sc.) and Ph.D. degrees in electronic engineering from Politecnico di Torino, Turin, Italy, in 1988 and 1993, respectively.

From 1991 to 1998, he was an Assistant Professor with the Department of Electronics, Politecnico di Torino. In 1998, he joined Politecnico di Milano, Milan, Italy, where he is currently a Full Professor of circuit theory and electromagnetic compatibility (EMC) with the Department of Electronics, Information, and Bioengineering. From 2015 to 2020, he served as the Chair for the B.Sc. and M.Sc. Study Programmes in electrical engineering. He is the author or coauthor of more than 220 papers published in international journals and conference proceedings. His research interests include EMC and field-to-wire coupling and crosstalk, conducted immunity and emissions in multi-wire structures, statistical techniques for EMC prediction, and experimental procedures and setups for EMC testing. His research activity is mainly related to the aerospace, automotive, energy, and railway industry sectors. He was a co-recipient of the 2005, 2016, and 2021 IEEE EMC Society Transactions Prize Paper Award and the IEEE EMC Society Technical Achievement Award in 2011. He is currently an Associate Editor for IEEE TRANSACTIONS ON ELECTROMAGNETIC COMPATIBILITY. From 2010 to 2015, he served as the IEEE EMC Society Chapter Coordinator. From 2007 to 2009, he was the Chair of the IEEE Italy Section EMC Society Chapter. He served as the Italian URSI Officer for Commission E (Electromagnetic Noise and Interference), from 2015 to 2018. He has been the Technical Program Chair of the ESA Workshop on Aerospace EMC, since 2009, and a member of the Technical Program Committee of the Asia Pacific International Symposium on EMC, since 2010.

Open Access funding provided by 'Politecnico di Milano' within the CRUI CARE Agreement